

MATHEMATISCHES FORSCHUNGSINSTITUT OBERWOLFACH

Report No. 45/2016

DOI: 10.4171/OWR/2016/45

Theory and Numerics of Inverse Scattering Problems

Organised by

Fioralba Cakoni, Piscataway

Martin Hanke-Bourgeois, Mainz

Andreas Kirsch, Karlsruhe

William Rundell, College Station

18 September – 24 September 2016

ABSTRACT. This workshop addressed specific inverse problems for the time-harmonic Maxwell's equations, resp. special cases of these, such as the Helmholtz equation or quasistatic approximations like in impedance tomography. The inverse problems considered include the reconstruction of obstacles and/or their material properties in a known background, given various kinds of data, such as near or far field measurements in the scattering context and boundary measurements in the quasistatic case.

Mathematics Subject Classification (2010): 35J05, 31B20, 65N20.

Introduction by the Organisers

Inverse scattering problems are of fundamental practical relevance, as the sensing of scattered waves is one of our most profound interactions with our neighborhood. Extracting information about the unknown medium or the force that is generating the scattered wave is often also a question of high economical value.

To address these problems basic mathematical questions need to be answered, including, for example, the following ones:

- What data are required to determine the shape of a scattering object (uniqueness problem)?
- Is there a constructive method to do so?

This workshop brought together 26 participants from seven different countries from all over the world, including both renowned international experts as well as promising young postdocs and PhD students. The contributed presentations were

mostly dealing with inverse scattering problems and electrical impedance tomography, but there also have been talks on related topics such as elastodynamics and optical coherence tomography. Although the primary focus of the meeting was on inverse problems there have also been contributed talks on the proper (well-posed) formulation of the associated direct or forward problems, and on corresponding existence and uniqueness theorems.

The majority of talks was addressing latest progress for the classical inverse obstacle scattering problem, which comes in various flavors depending on the material properties of the scatterer. These material properties can affect the boundary conditions as well as the index of refraction in the interior of the scatterer. Concerning the latter, a previous Oberwolfach meeting in 2012 had boosted the momentum of the theoretical investigation of so-called *transmission eigenvalues*, i.e., specific frequencies at which a certain obstacle or inhomogeneous medium is invisible for a given primary excitation. While the theory of this highly nonstandard eigenvalue problem was at its infancy at that meeting, there have meanwhile been many new developments in this area. A number of participants, being the main players in this area, gave fascinating insight into the possibilities that arise for the solution of the inverse problems from a computation of these (or related) eigenvalues from the data at hand. For the case of multiple scatterers alternative methods have been proposed to split the measured data into the corresponding components from the individual scatterers first, and then resort to any of the other methods for the full reconstruction.

As far as impedance tomography has been concerned a promising new technique was presented on how to see singularities of the conductivity with a backprojection type method, while another talk demonstrated the dramatic influence of using wrong assumptions about the geometry of the boundary of the object which is being imaged.

Two talks were drawing connections between classical regularization theory and inverse scattering and impedance tomography, respectively. In these presentations rigorous convergence proofs of the numerical reconstructions were discussed when the noise level in the data is going down to zero. Still, being severely ill-posed problems, the corresponding stability estimates are only of logarithmic type.

The meeting also saw an increasing number of contributions addressing (closed or open) wave guides. For the corresponding applications there are still fundamental problems in formulating and numerically solving the direct problems, but due to recent progress it is now possible to also rigorously address the associated inverse problems.

Having been a half-size workshop the schedule left enough space for very interesting and intensive discussions between and after the presentations. At three of the evenings some of the participants came with a glass of wine or beer to join spontaneously organized “informal presentations” of newly emerging fascinating inverse problems in different areas.

In the end all participants including those that could not present a talk for the lack of time agreed to have enjoyed a very special and informative meeting,

and we all look forward to reconvene at this wonderful spot for a similar event. Of course, the splendid support by service and staff was also responsible for this positive reception of the participants and the great success of this workshop.

Acknowledgement: The MFO and the workshop organizers would like to thank the National Science Foundation for supporting the participation of junior researchers in the workshop by the grant DMS-1049268, “US Junior Oberwolfach Fellows”. Moreover, the MFO and the workshop organizers would like to thank the Simons Foundation for supporting John Sylvester in the “Simons Visiting Professors” program at the MFO.

Workshop: Theory and Numerics of Inverse Scattering Problems

Table of Contents

Rainer Kress (joint with Fioralba Cakoni) <i>Inverse obstacle scattering with a generalized impedance boundary condition</i>	2577
Houssem Haddar (joint with Thi Phong Nguyen) <i>Differential imaging for locally perturbed periodic layers</i>	2579
Thorsten Hohage (joint with Frederic Weidling) <i>Stability estimates and variational source conditions</i>	2580
Shari Moskow (joint with Fioralba Cakoni and Bojan Guzina) <i>Homogenization of a transmission problem</i>	2583
Jun Zou (joint with Y. T. Chow, K. Ito, B. Jin) <i>A unified framework of direct sampling methods for general inverse problems</i>	2585
Roland Griesmaier (joint with John Sylvester) <i>Uncertainty principles for far field patterns with applications to inverse source problems</i>	2587
John Sylvester (joint with Roland Griesmaier) <i>Evanescence and uncertainty principles in the inverse source problem</i> ..	2590
Guanghai Hu (joint with Johannes Elschner) <i>Uniqueness in inverse medium scattering problems</i>	2591
Andreas Kirsch (joint with Andreas Rieder) <i>Inverse problems for abstract evolution equations with applications in electrodynamics and elasticity</i>	2595
Virginia Selgas (joint with Peter Monk) <i>An inverse problem for a waveguide in the frequency and the time domain</i>	2595
Bastian Harrach (joint with Mach Nguyet Minh) <i>Towards combining optimization-based techniques with shape reconstruction methods in EIT</i>	2598
Nuutti Hyvönen (joint with Vesa Kaarnioja, Lauri Mustonen and Stratos Staboulis) <i>Polynomial surrogates and inaccurately known measurement configurations in electrical impedance tomography</i>	2601

Samuli Siltanen (joint with Allan Greenleaf, Matti Lassas, Matteo Santacesaria and Gunther Uhlmann)	
<i>Detecting inclusions within inclusions in electrical impedance tomography</i>	2602
David Colton	
<i>Stekloff eigenvalues in inverse scattering</i>	2605
Xiaodong Liu	
<i>A fast and robust sampling method in inverse acoustic scattering problems</i>	2606
Julian Ott (joint with A.S. Bonnet-ben-Dhia, S. Fliss, A. Tonnoir, C. Hazard)	
<i>Halfspace matching for 2D open waveguides</i>	2608
Liliana Borcea (joint with Josselin Garnier)	
<i>Analysis of electromagnetic waves in random media</i>	2610
Tilo Arens (joint with Felix Hagemann and Frank Hettlich)	
<i>Measuring electromagnetic chirality</i>	2611
Otmar Scherzer (joint with Peter Elbau, Leonidas Mindrinos)	
<i>The inverse electromagnetic scattering problem in OCT for anisotropic media</i>	2612
Isaac Harris (joint with Fioralba Cakoni, Housseem Haddar and Shari Moskow)	
<i>Parameter identification for complex materials using transmission eigenvalues</i>	2616
Armin Lechleiter (joint with Ruming Zhang)	
<i>The Bloch transform and scattering from locally perturbed periodic structures</i>	2619

Abstracts

Inverse obstacle scattering with a generalized impedance boundary condition

RAINER KRESS

(joint work with Fioralba Cakoni)

The use of generalized impedance boundary conditions (GIBC) in the mathematical modeling of wave propagation has gained considerable attention in the literature over the last decades. This type of boundary conditions is applied to scattering problems for penetrable obstacles to model them approximately by scattering problems for impenetrable obstacles in order to reduce the cost of numerical computations. We will consider boundary conditions that generalize the classical impedance boundary condition, which is also known as Leontovich boundary condition, by adding a term with a second order differential operator. As compared with the Leontovich condition, this wider class of impedance conditions provides more accurate models, for example, for imperfectly conducting obstacles (see [3, 4]).

To formulate the scattering problem, let D be a simply connected bounded domain in \mathbb{R}^2 with boundary ∂D of class $C^{4,\alpha}$ and denote by ν the unit normal vector to ∂D oriented towards the complement $\mathbb{R}^2 \setminus \overline{D}$. We consider the scattering problem to find the total wave $u = u^i + u^s \in H_{\text{loc}}^2(\mathbb{R}^2 \setminus \overline{D})$ satisfying the Helmholtz equation

$$\Delta u + k^2 u = 0 \quad \text{in } \mathbb{R}^2 \setminus \overline{D}$$

with positive wave number k and the generalized impedance boundary condition

$$\frac{\partial u}{\partial \nu} + ik \left(\lambda u - \frac{d}{ds} \mu \frac{du}{ds} \right) = 0 \quad \text{on } \partial D$$

where d/ds is the tangential derivative and $\mu \in C^1(\partial D)$ and $\lambda \in C^1(\partial D)$ are complex valued functions. The incident wave u^i is assumed to be a plane wave $u^i(x) = e^{ikx \cdot d}$ with a unit vector d describing the direction of propagation. The scattered wave u^s has to satisfy the Sommerfeld radiation condition

$$\lim_{r \rightarrow \infty} \sqrt{r} \left(\frac{\partial u^s}{\partial r} - ik u^s \right) = 0, \quad r = |x|,$$

uniformly with respect to all directions. The derivative for $u|_{\partial D} \in H^{3/2}(\partial D)$ with respect to arc length s in the boundary condition has to be understood in the weak sense.

The Sommerfeld radiation condition is equivalent to the asymptotic behavior of an outgoing cylindrical wave of the form

$$u^s(x) = \frac{e^{ik|x|}}{\sqrt{|x|}} \left\{ u_\infty(\hat{x}) + O\left(\frac{1}{|x|}\right) \right\}, \quad |x| \rightarrow \infty,$$

uniformly for all directions $\hat{x} = x/|x|$ where the function u_∞ defined on the unit circle \mathbb{S}^1 is known as the far field pattern of u^s . Besides the direct scattering

problem to determine the scattered wave u^s for a given incident wave u^i the two inverse scattering problems that we will consider are to determine the boundary ∂D , for given impedance functions, or the impedance coefficients μ and λ , for a given boundary, from a knowledge of the far field pattern u_∞ on S^1 for one or several incident plane waves. The first problem we will call the inverse shape problem and the second the inverse impedance problem.

For the solution of a related boundary value problem for the Laplace equation with a generalized impedance boundary condition Cakoni and Kress [2] have proposed a single-layer potential approach that leads to a boundary integral equation or more precisely a boundary integro-differential equation governed by a pseudo-differential operator of order one. We will extend this approach to the direct scattering problem. As to be expected, the single-layer approach fails when k^2 is an interior Dirichlet eigenvalue for the negative Laplacian in D and to remedy this deficiency we describe a modified approach by a combined single- and double-layer approach that leads to a pseudo-differential operator of order two. We then proceed with describing the numerical solution of the integro-differential equation via trigonometric interpolation quadratures and differentiation that lead to spectral convergence.

We begin our analysis of the inverse problems with reviewing two uniqueness results, one for the inverse impedance problem using three incident fields (see [2]) and one for the full inverse problem using infinitely many incident fields at one wave number (see [1]). Our solution method for the inverse impedance problem is based on the uniqueness proof and the method for the inverse shape problem is based on a nonlinear boundary integral equation method in the spirit of the method proposed by Johansson and Sleeman [5] for the Dirichlet boundary condition. In both cases we follow the approach for the Laplace equation as developed by Cakoni and Kress [2] and illustrate the feasibility by a couple of numerical examples.

REFERENCES

- [1] L. Bourgeois, N. Chaulat, and H. Haddar, *On simultaneous identification of a scatterer and its generalized impedance boundary condition*, SIAM J. Sci. Comput. **34** (2012), A1824–A1848.
- [2] F. Cakoni and R. Kress, *Integral equation methods for the inverse obstacle problem with generalized impedance boundary condition*, Inverse Problems **29** (2013), 015005.
- [3] M. Duruflé, H. Haddar, and P. Joly, *High order generalized impedance boundary conditions in electromagnetic scattering problems*, Comptes Rendus Physique **7** (2006), 533–542.
- [4] H. Haddar, P. Joly, and H.M. Nguyen, *Generalized impedance boundary conditions for scattering by strongly absorbing obstacles: the scalar case*. Math. Models Methods Appl. Sci, **15** (2005), 1273–1300.
- [5] T. Johansson and B. Sleeman, *Reconstruction of an acoustically sound-soft obstacle from one incident field and the far field pattern*, IMA Jour. Appl. Math. **72** (2007), 96–112.

Differential imaging for locally perturbed periodic layers

HOUSSEM HADDAR

(joint work with Thi Phong Nguyen)

We consider the problem of identifying and reconstructing the geometry of a defect inside a periodic layer from measurements of scattered waves at a fixed frequency. We first extend the applications of so-called sampling methods (Factorization Method [5] and the Generalized Linear Sampling Method [1, 3]) to the problem of finding the geometry of both the defect and the periodic background. We treat the scalar case where the defect is modeled with a change in the refractive index of the medium. Our main contribution is on the design of a new imaging functional capable of directly reconstructing the geometry of the defect. Our method is inspired by the sampling method proposed in [2] but does not rely on differential measurements. The idea is to exploit the periodicity of the background to introduce a differential imaging functional between periods with defects and periods without defects. This construction is possible by using the measurement operator associated with a single Floquet-Bloch mode. The latter is obtained by restricting the incident waves and the measurements of the scattered waves to those that have a fixed quasi-periodicity factor. Analyzing the properties of this operator and applying the GLSM theory necessitate the analysis of a new type of interior transmission problems. The latter point is the main difficulty that necessitate the technical assumption of truncating the domain in the periodicity directions with periodic boundary conditions and thus allowing the possibility of using discrete Floquet-Bloch transformation. We refer to [4] where the truncation is shown to be equivalent to a uniform semi-discretization of the direct problem with respect to the Floquet-Bloch variable. The 2D numerical experiments for synthetic data show that the new sampling method is capable of identifying the geometry of the defect even though the background is complex and cannot be accurately reconstructed.

REFERENCES

- [1] L. Audibert and H. Haddar, *A generalized formulation of the Linear Sampling Method with exact characterization of targets in terms of farfield measurements*, *Inverse Problems* **30**, **035011**, 2014.
- [2] L. Audibert, A. Girard and H. Haddar, *Identifying defects in an unknown background using differential measurements*. *Inverse Probl. Imaging*, 9(3), 2015.
- [3] F. Cakoni, D. Colton and H. Haddar, *Inverse Scattering Theory and Transmission Eigenvalues*, CBMS Series, **88**, SIAM publications 2016.
- [4] H. Haddar and T.P. Nguyen *A volume integral method for solving scattering problems from locally perturbed infinite periodic layers*, *Applicable Analysis*, pp.1-29, 2016.
- [5] A. Kirsch and N. Grinberg, *The Factorization Method for Inverse Problems*, Oxford University Press, Oxford, 2008.

Stability estimates and variational source conditions

THORSTEN HOHAGE

(joint work with Frederic Weidling)

Introduction. Inverse problems are often formulated as operator equations

$$(1) \quad F(f) = g$$

with an injective forward operator $F : D(F) \subset \mathbb{X} \rightarrow \mathbb{Y}$ between Hilbert or Banach spaces. For simplicity we will confine ourselves to the case of Hilbert spaces although many of the results can be generalized to Banach space settings. Typically, inverse problems are ill-posed in the sense that F^{-1} is not continuous. Let f^\dagger denote the unknown exact solution and $g^\delta \in \mathbb{Y}$ noisy data with noise level $\delta \geq \|g^\delta - F(f^\dagger)\|$. A commonly used method to obtain stable solutions to (1) is Tikhonov regularization

$$(2) \quad f_\alpha^\delta \in \operatorname{argmin}_{f \in D(F)} [\|F(f) - g^\delta\|^2 + \alpha\|f - \bar{f}\|^2]$$

with regularization parameter $\alpha > 0$ and initial guess $\bar{f} \in \mathbb{X}$. Here $\|F(f) - g^\delta\|^2$ could be replaced by a more general data fidelity term and $\|f - \bar{f}\|^2$ by a more general penalty term. The aim of regularization theory is to estimate the worst case error $\sup\{\|f_\alpha^\delta - f^\dagger\| : g^\delta \in \mathbb{Y}, \|F(f^\dagger) - g^\delta\| \leq \delta\}$ as $\delta \rightarrow 0$. Classically the worst case error has been studied under spectral source conditions

$$(3) \quad f^\dagger - \bar{f} \in \mathcal{R}(\varphi(F'[f^\dagger]^* F'[f^\dagger]))$$

where $\varphi : [0, \infty) \rightarrow [0, \infty)$ is some *index function* (i.e. continuous, increasing, and $\varphi(0) = 0$), and $\varphi(F'[f^\dagger]^* F'[f^\dagger])$ is understood in the sense of the spectral functional calculus. More recently, starting with [3], variational source conditions (VSCs) in the form of a variational inequality

$$(4) \quad \forall f \in D(F) : \quad \frac{1}{2}\|f^\dagger - f\|^2 \leq \|f - \bar{f}\|^2 + \|f^\dagger - \bar{f}\|^2 + \psi(\|F(f^\dagger) - F(f)\|^2),$$

or equivalently

$$\forall f \in D(F) : \quad 2\langle f^\dagger - \bar{f}, f^\dagger - f \rangle \leq \frac{1}{2}\|f^\dagger - f\|^2 + \psi(\|F(f^\dagger) - F(f)\|^2)$$

have been studied. Here ψ is a concave index function. As shown in [2], (4) implies the convergence rate $\|f_{\alpha_{\text{opt}}}^\delta - f^\dagger\|^2 \leq 8\psi(\delta^2)$ for (2) with an optimal choice α_{opt} of α . The same convergence rate can also be shown for regularized Newton methods and computable a-posteriori parameter choice rules (see [6]). Note that as opposed to (3), the VSC (4) does not involve a derivative of F , and hence no restrictive assumptions relating F and F' such as the tangential cone condition are needed, at least for Tikhonov regularization.

It is obvious that a VSC (4) for all f^\dagger in a smoothness class $K \subset D(F)$ implies the *conditional stability estimate*

$$\forall f_1, f_2 \in K : \quad \frac{1}{2}\|f_1 - f_2\|^2 \leq \psi(\|F(f_1) - F(f_2)\|^2).$$

However, the converse implication is not obvious.

Main lemma. The strength and weakness of source conditions is that they present a single assumption which can be used conveniently in convergence proofs for regularization methods. On the other hand, source conditions are often difficult to interpret. The reason is that they combine two different factors influencing the rate of convergence of regularization methods into a single condition: smoothness of the solution and the degree of ill-posedness of F . The following simple lemma from [5] expresses these factors as sufficient conditions for a VSC in terms of a family of (bounded linear projection) operators P_r . (Actually, the operators P_r can be arbitrary, but this is how they will be chosen below.)

Lemma 1. *Let \mathbb{X} be a Hilbert space and $f^\dagger \in \mathbb{X}$. Moreover, let $P_r : \mathbb{X} \rightarrow \mathbb{X}$ be a family of operators, indexed by r in some index set \mathcal{J} , and let $\kappa, \sigma : \mathcal{J} \rightarrow [0, \infty)$ be two functions and $C > 0$ a constant such that*

- (1) $\|(I - P_r)(f^\dagger - \bar{f})\| \leq \kappa(r)$ for all $r \in \mathcal{J}$, and $\inf_{r \in \mathcal{J}} \kappa(r) = 0$,
- (2) for all $f \in D(F)$ with $\|f^\dagger - f\| \leq 4\|f^\dagger - \bar{f}\|$ and all $r \in \mathcal{J}$ we have

$$\langle P_r(f^\dagger - \bar{f}), f^\dagger - f \rangle \leq \sigma(r)\|F(f) - F(f^\dagger)\| + C\kappa(r)\|f - f^\dagger\|.$$

Then the VSC (4) holds true with the concave index function

$$\psi(t) := 2 \inf_{r \in \mathcal{J}} \left[(C + 1)^2 \kappa(r)^2 + \sigma(r) \sqrt{t} \right].$$

Note that the second assumptions (with $C = 0$) describes the growth of Lipschitz stability constants on (finite dimensional) subspaces.

Linear inverse problems. Suppose first that $T = F : \mathbb{X} \rightarrow \mathbb{Y}$ is bounded and linear. Then Lemma 1 with the spectral projection $P_r = 1_{[r, \infty)}(T^*T)$, $r > 0$ as well as results from [1, 7] yield the following result shown in [5]:

Theorem 2. *Let $f^\dagger \neq 0$, $\bar{f} = 0$, and consider estimators f_α^δ defined by (iterated) Tikhonov regularization, Landweber iteration, Lardy's or Showalter's method. Moreover, let φ be an index function for which $t \mapsto t^{\mu-1}\varphi(t)^2$ is decreasing for some $\mu \in (0, 1)$, and φ^2 is concave. Moreover, define*

$$\psi(t) := \varphi \left(\Theta^{-1}(\sqrt{t}) \right)^2 \quad \text{with} \quad \Theta(\lambda) := \sqrt{\lambda} \varphi(\lambda).$$

Then the following statements are equivalent:

- (1) f^\dagger satisfies the VSC (4).
- (2) $\sup_{r>0} \varphi(r)^{-1} \|(I - P_r)f^\dagger\| < \infty$.
- (3) $\sup_{\delta>0} \frac{1}{\psi(\delta)} \sup_{\|g^\delta - T f^\dagger\| \leq \delta} \inf_{\alpha>0} \|f_\alpha^\delta - f^\dagger\| < \infty$.

In other words, the VSC is not only sufficient for the convergence rate ψ (with optimal choice of α), but even necessary. In contrast, the corresponding spectral source conditions (3) are only sufficient. The conditions on φ exclude Hölder source conditions $\varphi(t) = t^\nu$ with $\nu \geq 1/2$.

For a number of interesting inverse problems including the backward and sideways heat equation, satellite gradiometry, and elliptic pseudodifferential operators,

both VSCs and spectral source conditions for certain φ, ψ can be interpreted in terms of Besov spaces. In all such cases we have

$$(5) \quad (3) \Leftrightarrow f^\dagger \in B_{2,2}^s = W_2^s, \quad \text{VSC (4)} \Leftrightarrow f^\dagger \in B_{2,\infty}^s.$$

In particular, on an interval the difference set $B_{2,\infty}^{1/2}([0,1]) \setminus B_{2,2}^{1/2}([0,1])$ contains piecewise smooth function with jumps. If we try to describe the smoothness of such functions in terms of spectral source conditions or equivalently Sobolev spaces, we never obtain the optimal rate, whereas the use of VSCs or equivalently Besov-Nikol'skiĭ-spaces does yield the optimal rate.

Inverse medium scattering problems. Let us consider the acoustic scattering problem described by the differential equation

$$(6) \quad \Delta u + {}^2 n(x)u = 0, \quad \text{in } \mathbb{R}^3$$

in combination with the Sommerfeld radiation condition, and suppose the contrast $f := 1 - n$ is supported in $B(\pi) := \{x \in \mathbb{R}^3 : |x| \leq \pi\}$. We first consider the near field problem described by the forward operator $F : H_0^m(B(\pi)) \rightarrow L^2(\partial B(R)^2)$, $R > \pi$, mapping f to the Green's function of (6) restricted to $\partial B(R)^2$. Again using Lemma 1 as well as Complex Geometrical Optics solutions, the following result has been shown in [4]:

Theorem 3. *Suppose $\frac{3}{2} < m < s$, $s \neq 2m + 3/2$ and f^\dagger satisfies $\|f^\dagger\|_{B_{2,\infty}^s} \leq C_s$ for some $C_s \geq 0$. Then a VSC (4) holds true with*

$$\psi(t) := A (\ln(3 + t^{-1}))^{-2\mu}, \quad \mu := \min \left\{ 1, \frac{s-m}{m+3/2} \right\}$$

where the constant $A > 0$ depends only on m, s, C_s, κ , and R .

Similar results have been shown for far field data ([4]) and for electromagnetic medium scattering problems ([8]).

REFERENCES

- [1] V. Albani, P. Elbau, M.V. de Hoop, O. Scherzer, *Optimal convergence rates results for linear inverse problems in Hilbert spaces*, Numer. Funct. Anal. Optim. **37** (2016), 521–540.
- [2] M. Grasmair, *Generalized Bregman distances and convergence rates for non-convex regularization methods*, Inverse Problems bf26 (2010), 115014 (16p.).
- [3] B. Hofmann, B. Kaltenbacher, C. Pöschl, and O. Scherzer, *A convergence rates result for Tikhonov regularization in Banach spaces with non-smooth operators*, Inverse Problems **23** (2007), 987–1010.
- [4] T. Hohage, F. Weidling, *Verification of a variational source condition for acoustic inverse medium scattering problems*, Inverse Problems **31** (2015), 075006 (14pp).
- [5] T. Hohage, F. Weidling, *Characterizations of variational source conditions, converse results, and maxisets of spectral regularization methods*, SIAM J. Numer. Anal. under revision, arXiv:1603.05133.
- [6] T. Hohage, F. Werner, *Iteratively regularized Newton-type methods for general data misfit functionals and applications to Poisson data*, Numer. Math. **123** (2013), 745–779.
- [7] A. Neubauer, *On converse and saturation results for Tikhonov regularization of linear ill-posed problems*, SIAM J. Numer. Anal. **34** (1997), 517–527.
- [8] F. Weidling, T. Hohage, *Variational source conditions and stability estimates for inverse electromagnetic medium scattering problems*, arXiv 1512.06586 (2015).

Homogenization of a transmission problem

SHARI MOSKOW

(joint work with Fioralba Cakoni and Bojan Guzina)

We study the homogenization of a transmission problem arising in the scattering theory for bounded inhomogeneities with periodic coefficients modeled by the anisotropic Helmholtz equation. The coefficients are assumed to be periodic functions of the fast variable, specified over the unit cell with characteristic size ϵ . By way of multiple scales expansion, we focus on the $O(\epsilon^k)$, $k = 1, 2$ bulk and boundary corrections of the leading-order ($O(1)$) homogenized transmission problem. The analysis in particular provides the H^1 and L^2 estimates of the error committed by the first-order-corrected solution considering i) bulk correction only, and ii) boundary and bulk correction. We treat explicitly the $O(\epsilon)$ boundary correction for the transmission problem when the scatterer is a unit square and show it has L^2 -limit as $\epsilon \rightarrow 0$, provided that the boundary cut-off of cells is fixed. We also establish the $O(\epsilon^2)$ -bulk correction describing the mean wave motion inside the scatterer. Our analysis also highlights a previously established, yet scarcely recognized fact that the $O(\epsilon)$ bulk correction of the mean motion vanishes identically.

More precisely, the scattering problem for an inhomogeneous obstacle D with periodically varying coefficients is formulated as a transmission problem for $u_\epsilon := u$ (the total field) in D and $u_\epsilon := u^s$ (the scattered field) in $\mathbb{R}^d \setminus \overline{D}$ as follows:

$$(1) \quad \begin{aligned} \nabla \cdot (a(x/\epsilon)\nabla u_\epsilon) + k^2 n(x/\epsilon)u_\epsilon &= 0 && \text{in } D \\ \Delta u_\epsilon + k^2 u_\epsilon &= 0 && \text{in } \mathbb{R}^d \setminus \overline{D} \\ u_\epsilon^+ - u_\epsilon^- &= f && \text{on } \partial D \\ (\nabla u_\epsilon \cdot \nu)^+ - (a(x/\epsilon)\nabla u_\epsilon \cdot \nu)^- &= g && \text{on } \partial D \end{aligned}$$

where u_ϵ satisfies the Sommerfeld radiation condition at infinity. The data is prescribed by the incident wave $f := u^i$ and $g := \nu \cdot \nabla u^i$ on ∂D , and the superscripts “+” and “−” denote the respective limits on ∂D from the exterior and interior of D . We follow along well known asymptotic theory for this problem as $\epsilon \rightarrow 0$. One expects the homogenized or limiting problem to read

$$(2) \quad \begin{aligned} \nabla \cdot (A\nabla u_0) + k^2 \bar{n}u_0 &= 0 && \text{in } D \\ \Delta u_0 + k^2 u_0 &= 0 && \text{in } \mathbb{R}^d \setminus \overline{D} \\ u_0^+ - u_0^- &= f && \text{on } \partial D \\ (\nabla u_0 \cdot \nu)^+ - (A\nabla u_0 \cdot \nu)^- &= g && \text{on } \partial D \end{aligned}$$

where u_0 satisfies the Sommerfeld radiation condition at infinity; \bar{n} denotes the unit cell average of n , i.e.

$$\bar{n} = \int_Y n(y)dy,$$

and A is a constant-valued matrix given by the weighted averages

$$(3) \quad A_{ij} = \int_Y \left(a_{ij}(y) - a_{ik}(y) \frac{\partial \chi^j}{\partial y_k}(y) \right) dy,$$

using Einstein summation, and where $\chi^j(y)$ are the so-called cell functions which represent the Y -periodic solutions to

$$(4) \quad \frac{\partial}{\partial y_i} \left(a_{ij}(y) - a_{ik}(y) \frac{\partial \chi^j}{\partial y_k}(y) \right) = 0.$$

We prove the following estimates:

Theorem 1. *Let u_ϵ be the solution to (1), u_0 the solution to (2), $u^{(1)} = \sum \chi^j \frac{\partial u_0}{\partial x_j}$ the usual bulk correction and θ_ϵ the boundary corrector. Then for any ball B_R of radius $R > 0$ which contains D ,*

$$\|u_\epsilon - (u_0 + \epsilon u^{(1)} + \epsilon \theta_\epsilon)\|_{L^2(B_R)} \leq C_R \epsilon^2 \|u_0\|_{H^4(D)}$$

and

$$\|u_\epsilon - (u_0 + \epsilon u^{(1)} + \epsilon \theta_\epsilon)\|_{H^1(D)} + \|u_\epsilon - (u_0 + \epsilon \theta_\epsilon)\|_{H^1(B_R \setminus D)} \leq C_R \epsilon^{3/2} \|u_0\|_{H^4(D)}$$

where the constant C_R is independent of ϵ and u_0 .

The first order boundary corrector function θ_ϵ is the solution to

$$(5) \quad \begin{aligned} \nabla \cdot a(x/\epsilon) \nabla \theta_\epsilon + k^2 n(x/\epsilon) \theta_\epsilon &= 0 \quad \text{in } D \\ \Delta \theta_\epsilon + k^2 \theta_\epsilon &= 0 \quad \text{in } \mathbb{R}^d \setminus \overline{D} \\ \theta_\epsilon^+ - \theta_\epsilon^- &= u^{(1)} \quad \text{on } \partial D \\ (\nabla \theta_\epsilon \cdot \nu)^+ - (a(x/\epsilon) \nabla \theta_\epsilon \cdot \nu)^- &= \left(\frac{v_0 - \bar{v}_0}{\epsilon} + v^{(1)} \right) \cdot \nu \quad \text{on } \partial D \end{aligned}$$

with Sommerfeld radiation conditions at infinity, and where v_0 and $v^{(1)}$ are standard bulk terms in the asymptotic expansion of $a(x/\epsilon) \nabla u_\epsilon$. For the case when the scatterer D is a square and the period cell is always cut by the boundary in the same way, we describe the boundary corrector limit θ^* . If we view instead a simplified θ_ϵ (the actual θ_ϵ is just a sum of eight similar functions, two corresponding to the data on each edge of D),

$$(6) \quad \begin{aligned} \nabla \cdot a(x/\epsilon) \nabla \theta_\epsilon + k^2 n(x/\epsilon) \theta_\epsilon &= 0 \quad \text{in } D \\ \Delta \theta_\epsilon + k^2 \theta_\epsilon &= 0 \quad \text{in } \mathbb{R}^2 \setminus \overline{D} \\ \theta_\epsilon^+ - \theta_\epsilon^- &= \chi^1(x/\epsilon) \frac{\partial u_0}{\partial x_1} \quad \text{on } \partial D \cap \{x_1 = 1\} \\ \theta_\epsilon^+ - \theta_\epsilon^- &= 0 \quad \text{on } \partial D \setminus \{x_1 = 1\} \\ (\nabla \theta_\epsilon \cdot \nu)^+ - (a(x/\epsilon) \nabla \theta_\epsilon \cdot \nu)^- &= \frac{1}{\epsilon} g_1(x/\epsilon) \frac{\partial u_0}{\partial x_1} + \overline{v^{(1)}}^{\partial \Omega} \quad \text{on } \partial D \cap \{x_1 = 1\} \\ (\nabla \theta_\epsilon \cdot \nu)^+ - (a(x/\epsilon) \nabla \theta_\epsilon \cdot \nu)^- &= 0 \quad \text{on } \partial D \setminus \{x_1 = 1\} \end{aligned}$$

together with the Sommerfeld radiation condition at infinity and where

$$(7) \quad g_1(x/\epsilon) = a_{11}(x/\epsilon) - a_{1k}(x/\epsilon) \frac{\partial \chi^1}{\partial y_k}(x/\epsilon) - A_{11}.$$

Then we prove the theorem:

Theorem 2. *Let $D = (0, 1) \times (0, 1)$ be the unit square and let ϵ_k be a sequence approaching zero such that $\frac{1}{\epsilon_k} - \lfloor \frac{1}{\epsilon_k} \rfloor = \delta$ for all k . Then if θ_{ϵ_k} solves (6) for $\epsilon = \epsilon_k$, we have that $\theta_{\epsilon_k} \rightarrow \theta^*$ strongly in $L^2_{loc}(\mathbb{R}^2)$ where θ^* solves*

$$\begin{aligned} \nabla \cdot A \nabla \theta^* + k^2 \bar{n} \theta^* &= 0 \quad \text{in } D \\ \Delta \theta^* + k^2 \theta^* &= 0 \quad \text{in } \mathbb{R}^2 \setminus \bar{D} \\ (\theta^*)^+ - (\theta^*)^- &= \chi_1^* \frac{\partial u_0}{\partial x_1} \quad \text{on } \partial D \cap \{x_1 = 1\} \\ (\theta^*)^+ - (\theta^*)^- &= 0 \quad \text{on } \partial D \setminus \{x_1 = 1\} \\ (\nabla \theta^* \cdot \nu)^+ - (A \nabla \theta^* \cdot \nu)^- &= \overline{a_{12}(\delta, y_2) w(0, y_2)^-} \frac{\partial^2 u_0}{\partial x_1 \partial x_2} + \overline{v^{(1)}}^{\partial \Omega} \quad \text{on } \partial D \cap \{x_1 = 1\} \\ (\nabla \theta^* \cdot \nu)^+ - (A \nabla \theta^* \cdot \nu)^- &= 0 \quad \text{on } \partial D \setminus \{x_1 = 1\} \end{aligned}$$

where $w(y_1, y_2)$ is the unique solution on a doubly infinite strip to

$$\begin{aligned} \nabla_y \cdot a(y_1 + \delta, y_2) \nabla w &= 0 \quad \text{in } G^- \\ \Delta_y w &= 0 \quad \text{in } G^+ \\ w(0, y_2)^+ - w(0, y_2)^- &= \chi^1(y_2) - \chi_1^* \\ (8) \quad \partial_{y_1} w(0, y_2)^+ - a_{1i}(\delta, y_2) \partial_{y_i} w(0, y_2)^- &= g_1(y_2) \\ w &[0, 1] - \text{periodic in } y_2 \end{aligned}$$

There exists $\gamma > 0$ such that $e^{\gamma y_1} \nabla w \in L^2(G^+)$
and $e^{-\gamma y_1} \nabla w \in L^2(G^-)$.

which decays exponentially to zero in both zero directions (and χ^* is the only such constant for which doubly exponentially decaying w exists). The two halves of the strip are given by

$$G^+ = \{y_1 > 0; y_2 \in [0, 1]\}$$

and

$$G^- = \{y_1 < 0; y_2 \in [0, 1]\}.$$

We then go on to consider mean field effects, which do not appear at first order but appear in general for higher order terms in the expansion.

A unified framework of direct sampling methods for general inverse problems

JUN ZOU

(joint work with Y. T. Chow, K. Ito, B. Jin)

Direct sampling methods have been developed in recent few years and proved effective, robust and computationally less expensive for locating and determining the scattering objects or inhomogeneous inclusions in various ill-posed inverse problems, especially when the observation data is limited, e.g., when the data is

only available from one single incident field or for one single pair of Cauchy data. These methods were motivated by a class of sampling-type reconstruction methods that were developed to determine the location and shape of the scattering objects approximately in inverse medium or obstacle scattering problems, such as linear sampling methods, factorization methods, point source method, and their many variants. These sampling-type methods were initiated by a simple method proposed by Colton and Kirsch in 1996 [5], and we refer to several systematic reviews and surveys on these methods and their developments in the monographs [1, 2, 5, 9, 10]. Compared with the traditional iterative-type or optimization-type reconstruction methods, these sampling methods are revolutionary and present many novel features: they are very easy to implement, no a priori information about the scattering objects is needed, no regularization parameters or stopping criteria need to be selected. But these sampling-type methods may be still computationally expensive, sufficient amount of data may be required in order to generate a reasonable reconstruction, and it may not be easy to determine appropriate cut-off values of the related indicator functions numerically. Considering the limitations of these sampling-type methods, direct sampling methods were proposed and investigated. They were developed first for wave type inverse problems [6, 8, 7, 11], then have been extended for solving other nonlinear severely ill-posed non-wave type inverse problems in recent years [3, 4], including the reconstruction of stationary and unstationary inclusions. In this talk, we discussed a general framework to unify the existing effective and robust direct sampling methods for both wave-type and non-wave type nonlinear inverse problems, such as inverse acoustic and electromagnetic scattering problems, electric impedance tomography and diffusive optical tomography problems, etc. We presented the motivations, derivations and justifications of direct sampling methods for some representative inverse problems, then discussed their unified general framework. Numerical simulations were shown to demonstrate the effectiveness and robustness of these methods for various inverse problems.

REFERENCES

- [1] F. Cakoni and D. Colton, *A Qualitative Approach to Inverse Scattering Theory*, Applied Mathematical Sciences Vol. 188, Springer, 2014.
- [2] F. Cakoni, D. Colton, and P. Monk, *The Linear Sampling Method in Inverse Electromagnetic Scattering*, Philadelphia, SIAM, 2011.
- [3] Y. T. Chow, K. Ito, K. Liu and J. Zou, Direct sampling method for diffusive optical tomography, *SIAM J. Sci. Comput.* 37 (2015), A1658–A1684.
- [4] Y. T. Chow, K. Ito and J. Zou, A direct sampling method for electrical impedance tomography, *Inverse Problems* 30 (2014), 095003 (25pp).
- [5] D. Colton and A. Kirsch, A simple method for solving inverse scattering problems in the resonance region, *Inverse Problems*, 12 (1996), 383–393.
- [6] R. Griesmaier, Multi-frequency orthogonality sampling for inverse obstacle scattering problems, *Inverse Problems*, 27 (2011), 085005.
- [7] K. Ito, B. Jin and J. Zou, A direct sampling method for inverse electromagnetic medium scattering, *Inverse Problems* 29 (2013) 095018.
- [8] K. Ito, B. Jin and J. Zou, A direct sampling method to an inverse medium scattering problem, *Inverse Problems* 28 (2012) 025003.

- [9] A. Kirsch and N. Grinberg, *The Factorization Method for Inverse Problems*, New York, Oxford University Press, 2008.
- [10] R. Potthast, *Point Sources and Multipoles in Inverse Scattering Theory*, Chapman & Hall, London 2001.
- [11] R. Potthast, A study on orthogonality sampling, *Inverse Problems*, 26 (2010), 074015.

Uncertainty principles for far field patterns with applications to inverse source problems

ROLAND GRIESMAIER
(joint work with John Sylvester)

We consider the following inverse problems for time-harmonic acoustic or electromagnetic wave propagation at a fixed frequency in two-dimensional free space:

- *Given the far field of a wave radiated by a collection of compactly supported sources, recover the far field components radiated by each of the individual sources separately.*
- *Given the far field radiated by a compactly supported source on most of the unit circle, restore the missing data segments.*

Although both inverse problems are severely ill-conditioned in general, we give precise conditions relating the wavelength, the diameters of the supports of the individual source components and the distances between them, and the size of the missing data segments, which guarantee that stable recovery in presence of noise is possible. The only additional requirement is that a priori information on the approximate location of the individual sources is available. Earlier works with related view points are, e.g., [2, 3].

To be more specific, let $f \in L_0^2(\mathbb{R}^2)$ be a compactly supported acoustic or electromagnetic source in the plane. The time-harmonic wave $u \in H_{\text{loc}}^1(\mathbb{R}^2)$ radiated by f at a fixed wave number $k > 0$ solves the Helmholtz equation

$$-\Delta u - k^2 u = k^2 f \quad \text{in } \mathbb{R}^2$$

together with the Sommerfeld radiation condition at infinity. Writing u in terms of the fundamental solution to the Helmholtz equation it follows immediately that the radiated field has the asymptotic behavior

$$u(x) = \frac{e^{i\pi/4}}{\sqrt{8\pi}} \frac{e^{ik|x|}}{\sqrt{k|x|}} u^\infty(\hat{x}) + \mathcal{O}(|x|^{-3/2}) \quad \text{for } |x| \rightarrow \infty,$$

where $\hat{x} := x/|x| \in S^1$. The far field u^∞ radiated by f is given by

$$u^\infty(\hat{x}) = k^2 \widehat{f}(k\hat{x}), \quad \hat{x} \in S^1,$$

i.e., it coincides with the Fourier transform of $k^2 f$ evaluated on the circle kS^1 .

An analysis of the singular values of the operator that maps sources supported in the ball $B_R(0)$ of radius R centered at the origin to their radiated far field, i.e.,

$$\mathcal{F}_{B_R(0)} : L^2(B_R(0)) \rightarrow L^2(S^1), \quad \mathcal{F}_{B_R(0)} f := k^2 \widehat{f}|_{kS^1},$$

shows that up to an L^2 -small error, a far field radiated by a limited power source in $B_R(0)$ is L^2 -close to a far field that belongs to the subspace of non-evanescent far fields, the span of $\{e^{in\theta}\}$ with $|n| \leq N$, where N is a little bigger than kR . Because the far field is a restricted Fourier transform, the formula for the Fourier transform of the translation of a function:

$$\widehat{f(\cdot + c)}(\theta) = e^{ic \cdot \theta} \widehat{f}(\theta), \quad \theta \in S^1, \quad c \in \mathbb{R}^2,$$

can be utilized to extend this observation to arbitrary balls $B_R(c)$ of radius R centered at $c \in \mathbb{R}^2$. We use T_c to denote the map from $L^2(S^1)$ to itself given by

$$T_c : \alpha(\theta) \mapsto e^{ikc \cdot \theta} \alpha(\theta).$$

Classical uncertainty principles in signal processing limit the amount of simultaneous concentration of a signal with respect to time and frequency (cf., e.g., [1]). The main ingredient in our analysis of far field splitting is the following theorem, which we call an uncertainty principle for the translation operator:

Theorem 1. *Let $\alpha, \beta \in L^2(S^1)$ such that the corresponding Fourier coefficients $\{\alpha_n\}$ and $\{\beta_n\}$ satisfy $\text{supp}\{\alpha_n\} \subset W_1$ and $\text{supp}\{\beta_n\} \subset W_2$ with $W_1, W_2 \subset \mathbb{Z}$, and let $c \in \mathbb{R}^2$. Then,*

$$|\langle T_c \alpha, \beta \rangle_{L^2(S^1)}| \leq \frac{\sqrt{|W_1| |W_2|}}{|kc|^{1/3}} \|\alpha\|_{L^2(S^1)} \|\beta\|_{L^2(S^1)}.$$

We use this uncertainty principle to show that the angle between translates of two far fields is bounded below when the translation parameter is large enough, so that we can split the sum of the two non-evanescent far fields into the original two summands.

We also make use of another uncertainty principle:

Theorem 2. *Let $\alpha, \beta \in L^2(S^1)$ such that the corresponding Fourier coefficients $\{\alpha_n\}$ satisfy $\text{supp}\{\alpha_n\} \subset W$ with $W \subset \mathbb{Z}$ and $\text{supp}\beta \subset \Omega$ with $\Omega \subset S^1$, and let $c \in \mathbb{R}^2$. Then,*

$$|\langle T_c \alpha, \beta \rangle_{L^2(S^1)}| \leq \sqrt{\frac{|W| |\Omega|}{2\pi}} \|\alpha\|_{L^2(S^1)} \|\beta\|_{L^2(S^1)}.$$

Corollaries of this theorem tell us that, if a far field is radiated from a small ball, and measured on most of the circle, then it is possible to recover its non-evanescent part on the entire circle.

To illustrate our findings, we consider a scattering problem with three obstacles as shown in figure 1 (left), which are illuminated by a plane wave $u^i(x) = e^{ikx \cdot d}$, $x \in \mathbb{R}$, with incident direction $d = (1, 0)$ and wave number $k = 1$. The scattered field u^s satisfies the homogeneous Helmholtz equation outside the obstacles, the Sommerfeld radiation condition at infinity, and it is well known that u^∞ can be written as a superposition of three far fields radiated by three individual smooth sources supported in arbitrarily small neighborhoods of the scattering obstacles. Figure 1 (right) shows the real part (solid line) and the imaginary part (dashed line) of the corresponding far field u^∞ .

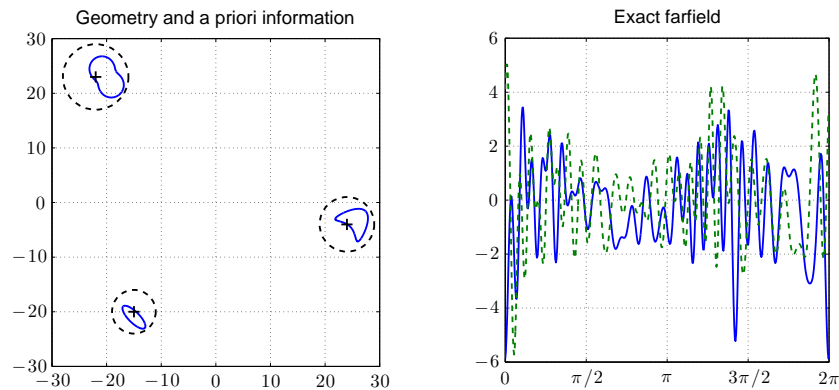


FIGURE 1. Left: Geometry of the scatterers (solid) and a priori information on the source locations (dashed). Right: Real part (solid) and imaginary part (dashed) of the far field.

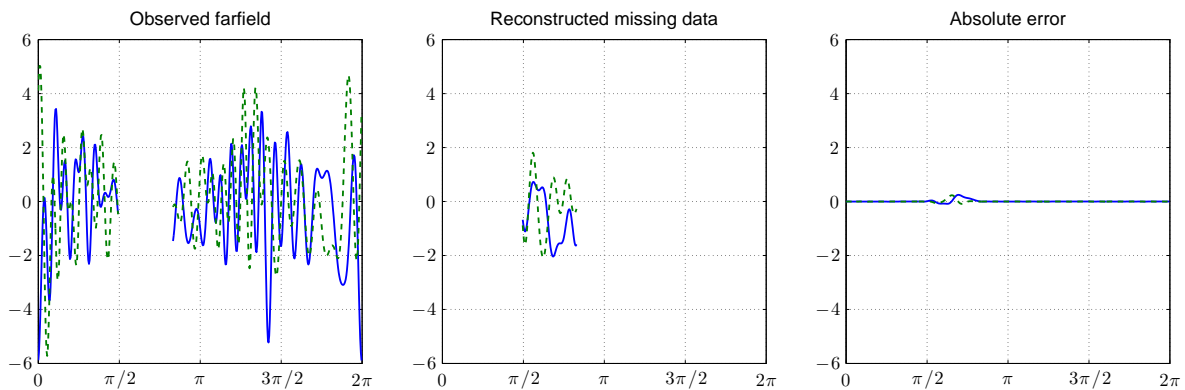


FIGURE 2. Left: Observed far field. Middle: Reconstruction of the missing part. Right: Difference between exact far field and reconstructed far field.

We assume that the far field cannot be measured on the segment

$$\Omega = \{\theta = (\cos t, \sin t) \in S^1 \mid \pi/2 < t < \pi/2 + \pi/3\},$$

and we apply a least squares procedure using the dashed circles shown in figure 1 (left) as a priori information on the approximate source locations. Figure 2 shows a plot of the observed data (left), of the reconstruction of the missing data segment obtained by the least squares algorithm (middle) and of the difference between the exact far field and the reconstructed far field (right). Again the solid line corresponds to the real part while the dashed line corresponds to the imaginary part.

For a complete description of the results outlined in this abstract we refer to [4].

REFERENCES

- [1] D. L. DONOHO AND P. B. STARK, Uncertainty principles and signal recovery, *SIAM J. Appl. Math.*, 49 (1989), 906–931.
- [2] R. Griesmaier, M. Hanke, and J. Sylvester, *Far field splitting for the Helmholtz equation*, *SIAM J. Numer. Anal.* **52** (2014), 343–362.
- [3] R. Griesmaier and J. Sylvester, *Far field splitting by iteratively reweighted ℓ^1 minimization*, *SIAM J. Appl. Math.* **76** (2016), 705–730.
- [4] R. Griesmaier and J. Sylvester, *Uncertainty principles for inverse source problems, far field splitting and data completion*, submitted.

Evanescence and uncertainty principles in the inverse source problem

JOHN SYLVESTER

(joint work with Roland Griesmaier)

The inverse source problem for the Helmholtz equation (time harmonic wave equation) seeks to recover information about a radiating source from remote observations of a monochromatic (single frequency) radiated wave measured far from the source (the far field). The two properties of far fields that we use to deduce information about shape and location of sources depend on the physical phenomenon of evanescence, which limits imaging resolution to the size of a wavelength, and the formula for calculating how a far field changes when the source is translated. We show how adaptations of *uncertainty principles* provide a very useful and simple tool for this kind of analysis.

Our version of an *uncertainty principle* is the following theorem:

Theorem 1. *Suppose that*

$$\begin{array}{ll} A : L^2 \mapsto L^2 & \text{supp} f \subset T \\ A^{-1} : L^1 \mapsto L^\infty & \text{supp} Af \subset W \end{array}$$

then

$$(1) \quad |(f, g)| \leq |T|^{\frac{1}{2}} |W|^{\frac{1}{2}} \|A\| \|A^{-1}\| \|f\|_2 \|g\|_2$$

We call this an uncertainty principle because, if we can set $g = f$ in (1), i.e. if there exists an f satisfying $\text{supp} f \subset T$ and $\text{supp} Af \subset W$, then (1) becomes

$$1 \leq |T|^{\frac{1}{2}} |W|^{\frac{1}{2}} \|A\| \|A^{-1}\|$$

In the case that A is the N -point DFT, this inequality becomes

$$N \leq |T| |W|$$

which is Theorem 1 in [1]. Our reformulation as an inner product is useful in cases where a single f that satisfies both support conditions does not exist. This is the case, for example, if the operator A is the Fourier transform or the operator which maps far fields (functions in $L^2(S^1)$ or $L^2(S^2)$) to their expansion in Fourier series or spherical harmonics.

Our main new application is to take $A = T_c$, where T_c is the far field translation operator, $\alpha(\Theta) \mapsto e^{ic \cdot \Theta} \alpha(\Theta)$, which represents the action induced by translation of a source f on its far field α , which is the Fourier transform of f restricted to the sphere of radius k .

We also show that we can combine different uncertainty principles to simultaneously complete data and split far fields from well-separated sources, in situations where it would not be possible to carry out either the data completion or the source splitting one after the other.

REFERENCES

- [1] D. L. DONOHO AND P. B. STARK, Uncertainty principles and signal recovery, *SIAM J. Appl. Math.*, 49 (1989), 906–931.

Uniqueness in inverse medium scattering problems

GUANGHUI HU

(joint work with Johannes Elschner)

Consider a time-harmonic acoustic wave incident onto a bounded penetrable scatterer $D \subset \mathbb{R}^n$ ($n = 2, 3$) embedded in a homogeneous isotropic medium. The incident field u^{in} is supposed to satisfy the Helmholtz equation

$$(1) \quad \Delta w + k^2 w = 0 \quad \text{in } \mathbb{R}^n,$$

with the wavenumber $k > 0$. It is supposed that u^{in} does not vanish identically and that the complement $D^e := \mathbb{R}^n \setminus \overline{D}$ of D is connected. The acoustic properties of the scatterer can be described by the refractive index function $q \in L^\infty(\mathbb{R}^n)$ such that $q \equiv 1$ in D^e . Hence, the contrast function $1 - q$ is supported in D . The wave propagation is then governed by the Helmholtz equation

$$(2) \quad \Delta u + k^2 q u = 0 \quad \text{in } \mathbb{R}^n.$$

In (2), $u = u^{in} + u^{sc}$ denotes the total wave where u^{sc} is the scattered field satisfying the Sommerfeld radiation condition, which leads to the asymptotic expansion

$$(3) \quad u^{sc}(x) = \frac{e^{ik|x|}}{|x|^{(n-1)/2}} u^\infty(\hat{x}) + \mathcal{O}\left(\frac{1}{|x|^{n/2}}\right), \quad |x| \rightarrow +\infty,$$

uniformly in all directions $\hat{x} := x/|x|$, $x \in \mathbb{R}^n$. The function $u^\infty(\hat{x})$ is an analytic function defined on \mathbb{S}^{n-1} and is referred to as the *far-field pattern* or the *scattering amplitude*. We consider the following two questions:

- (i): Does a penetrable obstacle scatter any incident wave trivially (that is, $u^s \equiv 0$) ?
- (ii): Does the far-field pattern of a single plane wave uniquely determine the shape of a penetrable obstacle ?

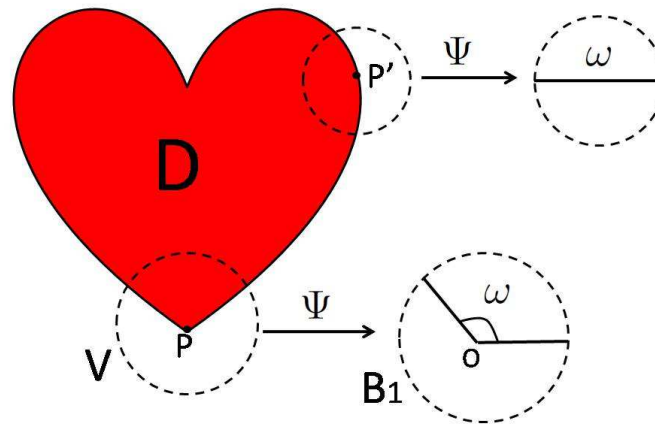


FIGURE 1. $P \in \partial D$ is a corner of the curvilinear polygon D , whereas P' is not a corner.

Define $\mathcal{K} = \mathcal{K}_\omega := \{(r, \theta) : r > 0, 0 < \theta < \omega\}$, a sector in \mathbb{R}^2 with the opening angle $\omega \in (0, 2\pi)$ at the origin. Denote by $B_a(P) := \{x \in \mathbb{R}^n : |x - P| < a\}$ the ball centered at P with radius $a > 0$, and by I the n -by- n identity matrix in $\mathbb{R}^{n \times n}$. For simplicity we write $B_a(O) = B_a$. We first introduce the concepts of (planar) corner points in \mathbb{R}^2 , and edge and circular conic points in \mathbb{R}^3 ; see Figure 1 for illustration of planar corners of a curvilinear polygon.

Definition 1. (see e.g., [7, Chapter 1.3.7]) Let D be a bounded open set of \mathbb{R}^2 . The point $P \in \partial D$ is called corner point if there exist a neighbourhood V of P , a diffeomorphism Ψ of class C^2 and an angle $\omega = \omega(P) \in (0, 2\pi) \setminus \{\pi\}$ such that

$$(4) \quad \nabla \Psi(P) = I \in \mathbb{R}^{2 \times 2}, \quad \Psi(P) = O, \quad \Psi(V \cap D) = \mathcal{K}_\omega \cap B_1.$$

We shall say that D is a curvilinear polygon, if for every $P \in \partial D$, (4) holds with $\omega(P) \in (0, 2\pi)$.

Definition 2. Let $D \subset \mathbb{R}^3$ be a bounded open set. The point $P \in \partial D$ is called a vertex if there exist a neighbourhood V of P , a diffeomorphism Ψ of class C^2 and a polyhedral cone Π with the vertex at O such that $\nabla \Psi(P) = I \in \mathbb{R}^{3 \times 3}$, $\Psi(P) = O$ and Ψ maps $V \cap \overline{D}$ onto a neighbourhood of O in $\overline{\Pi}$. P is called an edge point of D if

$$(5) \quad \Psi(V \cap D) = (\mathcal{K}_\omega \cap B_1) \times (-1, 1)$$

for some $\omega(P) \in (0, 2\pi) \setminus \{\pi\}$. We shall say that D is a curvilinear polyhedron if, for every point $P \in \partial D$, either (5) applies with $\omega(P) \in (0, 2\pi)$ or $P \in \partial D$ is a vertex.

A curvilinear polygon resp. polyhedron allows both curved and flat surfaces near a corner resp. edge point (see Figure 1). The conditions (4) and (5) exclude peaks at O (for which the opening angle of the planar sector is 0 or 2π).

Let $\mathcal{C} = \mathcal{C}_\omega$ be an infinite circular cone in \mathbb{R}^3 defined as

$$(6) \quad \mathcal{C} := \{(r, \theta, \varphi) : r > 0, 0 < \theta < \omega, 0 \leq \varphi < 2\pi\}$$

for some $\omega \in (0, \pi) \setminus \{\pi/2\}$.

Definition 3. We say that a bounded open set $D \subset \mathbb{R}^3$ has a circular conic point $P \in \partial D$ if $D \cap B_a(P)$ coincides with $\mathcal{C} \cap B_a$ for some $a > 0$ up to a coordinate translation or rotation. D is called a circular conical domain if it has at least one circular conic point.

Let D be a bounded penetrable obstacle in \mathbb{R}^n , with $O \in \partial D$ being a planar corner point in \mathbb{R}^2 , and an edge or circular conic point in \mathbb{R}^3 . Denote by $W^{\kappa,p}$ and $H^\kappa = W^{\kappa,2}$ the standard Sobolev spaces. We make the following assumption on q in a neighborhood of O .

Assumption (a). There exist $l \in \mathbb{N}_0$, $s \in (0, 1)$, $\epsilon > 0$ such that

$$(7) \quad q \in C^{l,s}(\overline{D} \cap B_\epsilon) \cap W^{l,\infty}(B_\epsilon), \quad \nabla^l(q-1) \neq 0 \quad \text{at } O.$$

By the Assumption (a), q is required to be $C^{l,s}$ continuous up to the boundary only in a neighborhood of O . The relation (7) with $l = 0$ means the discontinuity of q at O , i.e., $q(O) \neq 1$, and has been assumed in [8, 1, 2, 4] in combination with other smoothness conditions on $q|_{\overline{D}}$ near O . A piecewise constant potential such that $q|_{\overline{D}} \equiv q_0 \neq 1$ fulfills the Assumption (a) with $l = 0$. When $l \geq 1$, it follows from the Sobolev imbedding relation $W^{l,\infty}(B_\epsilon) \subset C^{l-1}(B_\epsilon)$ that the function q is C^{l-1} -smooth in B_ϵ , implying that $q(x) = 1 + \mathcal{O}(|x|^l)$ as $|x| \rightarrow 0$ in D . Physically, this means a lower contrast of the material on $\overline{D} \cap B_\epsilon$ compared to the background medium.

The main results of this paper are stated as follows.

Theorem 4. Under the Assumption (a), a penetrable obstacle with a planar corner point in \mathbb{R}^2 , and with an edge or a circular conic point in \mathbb{R}^3 scatters every incident wave non-trivially.

Theorem 5. Let D_j ($j = 1, 2$) be two penetrable obstacles in \mathbb{R}^n ($n = 2, 3$). Suppose that the potentials q_j associated to D_j fulfill the Assumption (a) for each corner, edge and circular conic point. If ∂D_2 differs from ∂D_1 in the presence of a corner, edge or circular conic point lying on the boundary of the unbounded component of $\mathbb{R}^n \setminus (\overline{D_1 \cup D_2})$, then the far-field patterns corresponding to D_j and q_j incited by any incoming wave cannot coincide.

Corollary 6. If the potential fulfills the Assumption (a) near each corner resp. vertex, then the shape of a convex penetrable polygon resp. polyhedron with flat sides can be uniquely determined by a single far-field pattern.

Our approach relies on the singularity analysis of the inhomogeneous Laplace equation in a cone (see e.g., [5, 7]).

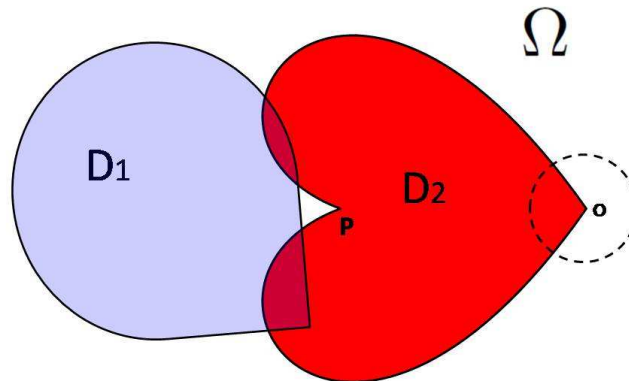


FIGURE 2. D_1 and D_2 cannot generate the same far-field pattern due to the presence of the corner point $O \in (\partial D_2 \setminus \partial D_1) \cap \partial \Omega$, where Ω is the unbounded component of $\mathbb{R}^2 \setminus (D_1 \cup D_2)$. The corner point P lies on $\partial D_2 \setminus \partial D_1$, but $P \notin \partial \Omega$.

REFERENCES

- [1] E. Blåsten, L. Päiväranta and J. Sylvester, Corners always scatter, *Commun. Math. Phys.*, 331 (2014): 725–753.
- [2] J. Elschner and G. Hu, Corners and edges always scatter, *Inverse Problems*, 31 (2015): 015003.
- [3] J. Elschner and G. Hu, Acoustic Scattering from Corners, Edges and Circular Cones, arXiv:1603.05186 .
- [4] G. Hu, M. Salo, E. V. Vesalainen, Shape identification in inverse medium scattering problems with a single far-field pattern, *SIAM J. Math. Anal.*, 48 (2016): 152–165.
- [5] P. Grisvard, *Singularities in Boundary Value Problems*, Masson, Paris, 1992.
- [6] S. Kusiak and J. Sylvester, The scattering support, *Communications on Pure and Applied Mathematics*, 56 (2003): 1525–1548.
- [7] V. G. Maz'ya, S. A. Nazarov and B. A. Plamenevskii, *Asymptotic Theory of Elliptic Boundary Value Problems in Singularly Perturbed Domains Volume I*, Birkhäuser-Verlag, Basel, 2000.
- [8] L. Päiväranta, M. Salo and E. V. Vesalainen, Strictly convex corners scatter, arXiv:1404.2513, 2014.

Inverse problems for abstract evolution equations with applications in electrodynamics and elasticity

ANDREAS KIRSCH

(joint work with Andreas Rieder)

It is common knowledge – mainly based on experience – that parameter identification problems for partial differential equations are ill-posed. We model parameter identification problems for abstract evolution equations by introducing an additional (bounded) operator in the equation and present a general theory which explains not only the local ill-posedness of the corresponding inverse problem but also provides the Frechét derivative of the parameter-to-solution map and its adjoint which is needed, e.g., in Newton like solvers. Our abstract results are applied to the standard parameter identification problems for Maxwell's equations and the elastic wave equation. By the concept of mild solutions we were able to weaken the assumptions on the parameters considerably.

The talk is based on the recent article [1]

REFERENCES

- [1] A. Kirsch and A. Rieder, *Inverse Problems for Abstract Evolution Equations with Applications in Electrodynamics and Elasticity*, *Inverse Problems* 32 (2016).

An inverse problem for a waveguide in the frequency and the time domain

VIRGINIA SELGAS

(joint work with Peter Monk)

We consider the problem of locating and imaging an obstacle in a sound-hard infinite tubular waveguide from measurements of the scattered field for point sources and receivers placed on a pair of surfaces located inside the waveguide. To deal with this problem, the Linear Sampling Method (LSM) was already used in [1] for detecting sound-soft obstacles. The assumption therein of a sound hard-pipe is in accordance with the application we have in mind, which is the use of acoustic techniques to inspect underground pipes such as sewers.

First, we study the frequency domain inverse problem for detecting a penetrable obstacle which may lie on the walls of the pipe. We analyze both the forward problem and the associated interior transmission problem, which we use to adapt and analyze the LSM and the Reciprocity Gap Method (RGM) to deal with this inverse problem. We also study the relationship between these two methods, showing that the RGM can be understood as a generalized LSM where the sources and receivers are placed on different surfaces.

Next, we consider the inverse problem in the time domain. Under the assumption that the obstacle is impenetrable, we adapt and analyze the Time Domain Linear Sampling Method (TD-LSM) to the waveguide problem. This involves

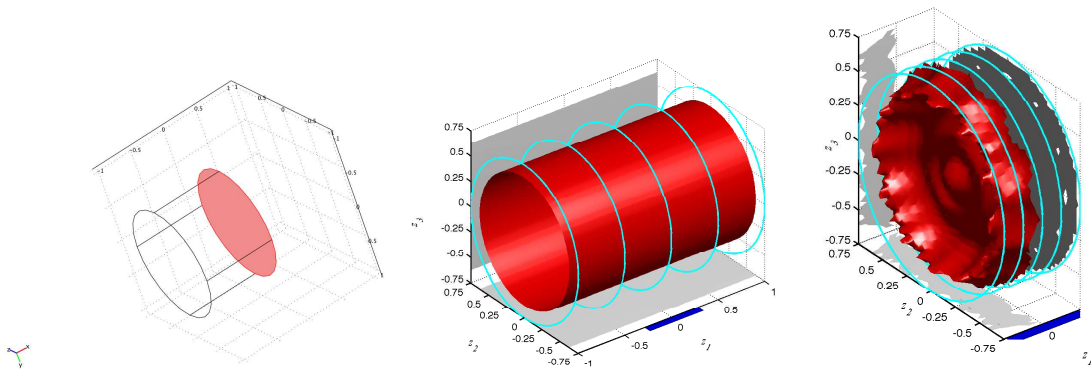
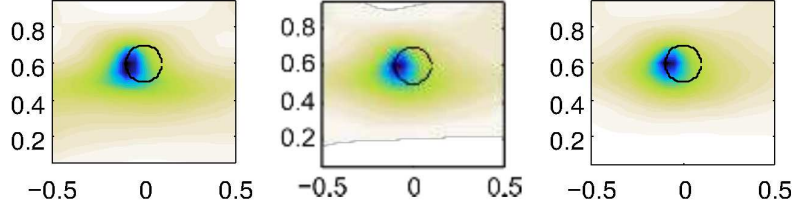


FIGURE 1. Blocked pipe, 6KHz: Exact object (left panel), and LSM reconstructions with distant (central panel) or near (right panel) measurements. The method fails to detect the end of the pipe using measurements far from the blockage (central panel) and succeeds for close measurements (right panel).

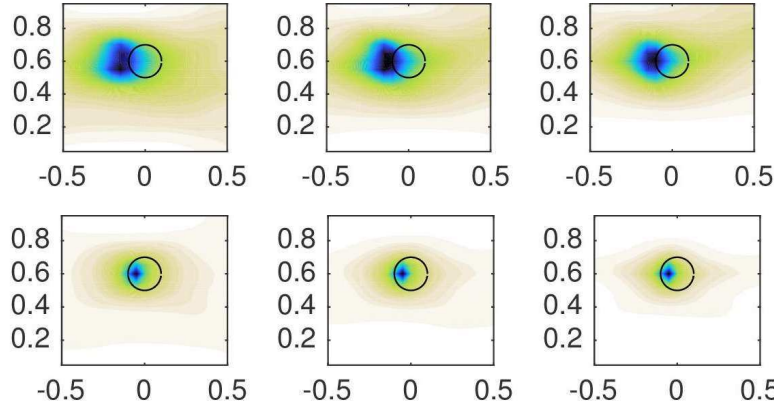
proving new time domain estimates for the forward problem, as well as analyzing several time domain operators arising in the inversion scheme.

For both the frequency and time domain inverse problems, we present numerical results which confirm the expected behaviour of the methods under study; in particular, and as expected, the TD-LSM improves the image reconstructed by the LSM for a suitable choice of the time modulation of the incident wave; see [5].

In this talk, we focus on the difficulties inherent in using waves travelling along waveguides. On one hand, for the frequency domain case, we showed in [4] that the LSM did not detect a completely blocked three-dimensional pipe. Although this situation was not covered by our theory, we found it to be (as far as we were aware) the first example where the LSM or RGM failed completely to detect a scatterer; see Fig.1 (central panel). Later, we investigated a modal solution of the blocked pipe, which suggests the necessity of using some evanescent modes to detect the end of the pipe. This is in good agreement with our new numerical results, where we move the measurement surface closer to the blockage in order to capture some evanescent modes, which do allow us to detect the blockage; see Fig.1 (right panel). On the other hand, in the time domain, we found in [5] that a standard Gaussian modulated input pulse requires very long simulation times (and hence computing time is too long). For example, when we considered a two-dimensional waveguide with unit height and a target occupying a circle of radius 0.1 centered at (0,0.6), we were able to compute sufficient forward data to resolve an obstacle when the transducers were close to the obstacle (on $x_1 = -2$), but not when they were further away (on $x_1 = -5$); see the corresponding reconstructions on Fig.2 (top row). For those experiments, we chose the incident waves from point sources whose time shape was given by $\chi(t) = (-3.2 \sin(\omega t) t + \omega \cos(\omega t) + 9.6 \sin(\omega t)) \exp(-1.6(t - 3)^2)$, with central frequency $\omega = 10$ or 15. Following the ideas of [2], we have now considered a specially designed time profile $\xi(t) = \sum_{n=1}^5 \xi_n(t)$, where $\xi_n(t) = \frac{d}{dt}(\sin(A_n t) e^{-B_n(t - C_n)^2})$ and $A_n, B_n, C_n \in \mathbb{R}$ are



Contour plots of the indicator function for transducers close to the target, using the Gaussian modulated pulse $\chi(t)$



Contour plots of the indicator function for transducers near (above) or far (below) from the target, using the incident modulation $\xi(t)$ from [2]

FIGURE 2. Reconstructions of a small circle using measurements near (top and middle rows) or far (bottom row) from the obstacle. We investigate different choices of the time modulation of the sources ($\chi(t)$ in top row, and $\xi(t)$ in middle and bottom rows). Different columns correspond to different Tikhonov regularization parameters.

fixed to select the mean frequency and the support of the signal in the frequency domain. Indeed, choosing $A_n = \pi(n - 0.5) - \frac{4B_n}{\pi(n-0.5)}$, $B_n = \frac{\pi^2}{200}$ and $C_n = \frac{5}{\sqrt{2B_n}}$, each function $\xi_n(t)$ is such that the support of its Fourier-Laplace transform does not have significant amplitude at any of the cut-off frequencies corresponding to vanishing group velocities. Since these cut-off frequencies are avoided, the scattered fields in the time domain decrease quite rapidly to 0 when $t \rightarrow +\infty$. As shown in Fig.2 (middle and bottom rows), the usage of this time profile for the incident waves allows us to work within a reasonable final time of the forward computation that provides suitable synthetic data and, hence, obtain admissible reconstructions of the target.

The analysis of the TD-LSM when the obstacle touches the walls of the pipe, as well as the usage of experimental data, are to be studied in future.

REFERENCES

- [1] L. Bourgeois, E. Lunéville, *The Linear Sampling Method in a waveguide: a modal formulation*, *Inv. Prob.* **24**(1) (2008), pp. 015018.
- [2] V. Baronian, L. Bourgeois, A. Recoquillay, *Imaging an acoustic waveguide from surface data in the time domain*, *Wave Motion* **66** (2016), pp. 68–87.
- [3] L. Fan, P. Monk, V. Selgas, *Time dependent scattering in an acoustic waveguide via convolution quadrature and the Dirichlet-to-Neumann map*, *Trends in Differential Equations and Applications (SEMA-SIMAI Springer Series)* **8** (2016), pp. 321–337.
- [4] P. Monk, V. Selgas, *Sampling type methods for an inverse waveguide problem*, *Inverse Problems and Imaging* **6**(4) (2012), pp. 709–747.
- [5] P. Monk, V. Selgas, *An inverse acoustic waveguide problem in the time domain*, *Inverse Problems* **32** (2016), pp. 055001.

Towards combining optimization-based techniques with shape reconstruction methods in EIT

BASTIAN HARRACH

(joint work with Mach Nguyet Minh)

Electrical Impedance Tomography (EIT) is a newly emerging imaging method, where electrical currents are driven through an imaging subject to image its interior conductivity distribution. In the so-called continuum model, EIT leads to the mathematical inverse problem of recovering the coefficient function $\sigma \in L^{\infty}_{+}(\Omega)$ in

$$(1) \quad \nabla \cdot (\sigma(x)\nabla u(x)) = 0, \quad x \in \Omega,$$

from knowledge of the Neumann-Dirichlet operator

$$\Lambda(\sigma) : L^2_{\diamond}(\partial\Omega) \rightarrow L^2_{\diamond}(\partial\Omega), \quad g \mapsto u|_{\partial\Omega},$$

where $u \in H^1_{\diamond}(\Omega)$ solves (1) with $\sigma\partial_{\nu}u|_{\partial\Omega} = g$.

To alleviate modelling errors, one often compares measurements with that of a reference state σ_0 and aims to reconstruct the conductivity difference $\sigma - \sigma_0$ from noisy difference measurements

$$\Lambda^{\delta}_{\text{meas}} \approx \Lambda(\sigma) - \Lambda(\sigma_0).$$

A natural and generic approach is to linearize the difference measurements

$$\Lambda^{\delta}_{\text{meas}} \approx \Lambda(\sigma) - \Lambda(\sigma_0) \approx \Lambda'(\sigma_0)(\sigma - \sigma_0)$$

and to approximate the conductivity difference $\kappa \approx \sigma - \sigma_0$ by minimizing a linearized and regularized data-fit functional

$$(2) \quad \|\Lambda'(\sigma_0)\kappa - \Lambda^{\delta}_{\text{meas}}\|^2 + \text{regularization} \rightarrow \min!$$

Such algorithms are widely used in practice but their theoretical justification has remained an open question, and the choice of regularization is often heuristic.

For exact data ($\delta = 0$) and piecewise analytic conductivities σ and σ_0 , the result in [3] showed that a piecewise analytic solution κ of the linearized EIT equation

$$(3) \quad \Lambda'(\sigma_0)\kappa = \Lambda(\sigma) - \Lambda(\sigma_0)$$

fulfills

$$\text{supp}_{\partial\Omega}\kappa = \text{supp}_{\partial\Omega}(\sigma - \sigma_0),$$

where $\text{supp}_{\partial\Omega}$ denotes the outer support, i.e., the support together with all parts that cannot be reached from the boundary $\partial\Omega$ without crossing the support.

This result suggests that the generic optimization-based approach of minimizing the linearized data-fit functional (2) is capable of correctly determining shapes in the difference image, i.e., those parts of the domain where the conductivity σ differs from the reference value σ_0 . However, the result in [3] requires an exact solution of the linearized equation (3) with noiseless measurements in the continuum model. In a practical setting, one can only access a matrix of noisy voltage and currents measurements on finitely-many electrodes which can be regarded as a (finite-dimensional and noisy) approximation $\Lambda_{\text{meas}}^\delta$ to the idealized difference of Neumann-Dirichlet operators $\Lambda(\sigma) - \Lambda(\sigma_0)$. A crucial question is how to design a regularization strategy for the standard optimization-based approach (2) that ensures convergence of the reconstructed shapes in the limit of more and more precise measurements on more and more electrodes.

To develop such a regularization strategy we combine the standard optimization-based approach with the following novel monotonicity-based shape reconstruction technique based on [4]. To explain the basic idea assume that $\sigma_0 = 1$ and $\sigma = 1 + \chi_D$ where D denotes the outer support of the conductivity change. Let $P \subseteq \Omega$ denote a test domain, e.g. a pixel from the partition on which $\sigma - \sigma_0$ is to be reconstructed. The monotonicity method developed in [4] shows that

$$(4) \quad P \subseteq D \quad \text{if and only if} \quad \exists \alpha > 0 : \alpha \Lambda'(\sigma_0)\chi_P \geq \Lambda(\sigma) - \Lambda(\sigma_0),$$

where the monotonicity inequality on the right hand side of (4) is to be understood in the sense of definiteness of self-adjoint compact operators.

For the k -th pixel P_k we calculate the maximal constant $\beta_k \geq 0$ such that the monotonicity inequality on the right hand side of (4) holds true for all $\alpha \in [0, \beta_k]$. For noisy data $\Lambda_{\text{meas}}^\delta \approx \Lambda(\sigma) - \Lambda(\sigma_0)$ we regularize this quantitative monotonicity test by calculating the maximal constant $\beta_k^\delta \geq 0$ with

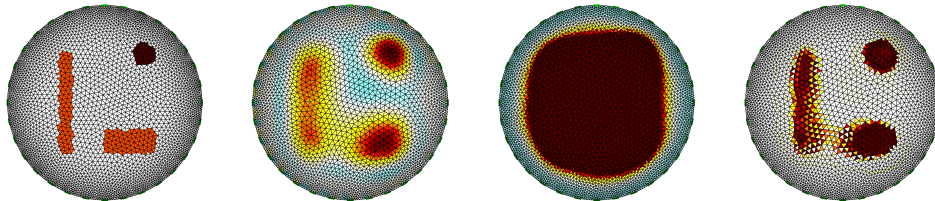
$$\beta_k^\delta \Lambda'(\sigma_0)\chi_P \geq \Lambda_{\text{meas}}^\delta - \delta I.$$

Note that in the numerical implementation, β_k^δ can be obtained from calculating the minimal eigenvalue of an auxiliary matrix as explained in [1, 2]. From the theory in [4] it follows that

$$\beta_k^\delta \rightarrow \beta_k, \quad \text{and} \quad \beta_k \text{ fulfills } \begin{cases} \beta_k = 0 & \text{if } P_k \not\subseteq D, \\ \beta_k \geq \frac{1}{2} & \text{if } P_k \subseteq D. \end{cases}$$

Hence, a plot of β_k will show the correct shape of D up to the resolution determined by the pixel partition, and, for noisy data, a plot of β_k^δ converges against the correct shape in the limit of $\delta \rightarrow 0$. However, in practice, the reconstructions tend to be very sensitive to noise, cf. the example with 1% noise in figure 1 where the result of the standard heuristic linearized method (for which no convergence results are known) shown in the second image is clearly better than the result from the rigorously justified monotonicity method shown in the third image.

FIGURE 1. True conductivity (left image) and reconstructions obtained with a standard linearized method with Tikhonov regularization (2nd image), the monotonicity method (3rd image), and the monotonicity-regularized linearized method (4th image) using data with 1% relative noise.



To improve the practical performance of the monotonicity method without loosing its rigorous convergence properties we combine the monotonicity-based approach with the standard optimization-based approach (2). We minimize

$$(5) \quad \|\Lambda'(\sigma_0)\kappa - (\Lambda(\sigma) - \Lambda(\sigma_0))\|^2 \rightarrow \min!$$

under the constraint that κ is a non-negative function which is piecewise constant with respect to the pixel partition, and fulfills $\kappa|_{P_k} \leq \min\{\gamma, \beta_k\}$ on each pixel. For noisy data we minimize

$$(6) \quad \|\Lambda'(\sigma_0)\kappa - \Lambda_{\text{meas}}^\delta\|^2 \rightarrow \min!$$

under the constraint that $0 \leq \kappa|_{P_k} \leq \min\{\gamma, \beta_k^\delta\}$. The constant $\gamma > 0$ is determined from the minimal inclusion contrast according to the theory developed in [4] (e.g. $\gamma = 1/2$ for $\sigma = 1 + \chi_D$). For the functional in (5) we use a Frobenius norm of a finite-dimensional Galerkin projection of the Neumann-Dirichlet operators so that this is a convex minimization problem under box constraints.

Due to the definition of β_k the minimizer of (5) will be zero on each pixel which is not contained in the outer support of $\sigma - \sigma_0$. Moreover, it is shown in [2] that in each pixel contained in the outer support, $\beta_k \geq \gamma$ and raising the value of $\kappa|_{P_k}$, at least up to γ , will always lower the functional (5). Hence, the monotonicity-constrained minimizer of (5) will show the correct outer support up to the pixel partition. For noisy data it can be shown, see [2], that minimizers κ^δ of (6) exist and that $\kappa^\delta \rightarrow \kappa$. In that sense, we have succeeded in developing the first regularization strategy for the standard linearized residuum minimization algorithm for which convergence of the reconstructed shapes can be rigorously guaranteed. The fourth image in figure 1 shows that the monotonicity-regularized linearized method clearly outperforms the monotonicity method. For more numerical results and the mathematical details of the above arguments we refer to the recent publication [2].

REFERENCES

- [1] B. Harrach: *Interpolation of missing electrode data in electrical impedance tomography*, Inverse Problems **31** (2015), 115008.
- [2] B. Harrach, M. N. Minh: *Enhancing residual-based techniques with shape reconstruction features in Electrical Impedance Tomography*, Inverse Problems, accepted for publication.
- [3] B. Harrach, J. K. Seo: *Exact shape-reconstruction by one-step linearization in electrical impedance tomography*, SIAM Journal on Mathematical Analysis **42** (2010), 1505–1518.
- [4] B. Harrach, M. Ullrich: *Monotonicity-based shape reconstruction in electrical impedance tomography*, SIAM Journal on Mathematical Analysis **45** (2013), 3382–3403.

Polynomial surrogates and inaccurately known measurement configurations in electrical impedance tomography

NUUTTI HYVÖNEN

(joint work with Vesa Kaarnioja, Lauri Mustonen and Stratos Staboulis)

The objective of *electrical impedance tomography* (EIT) is to reconstruct the conductivity inside a physical body based on currents and voltages measured at a finite number of contact electrodes attached to the object boundary. The most accurate model for EIT is the *complete electrode model* (CEM) that accounts for the electrode shapes and the contact resistances at the electrode-object interfaces [5, 10]. For information on potential applications of EIT, we refer to the review articles [2, 4, 11] and the references therein.

In a real-world application of EIT, the conductivity is practically never the only unknown; the knowledge about the contact resistances, the electrode positions and the shape of the examined body is typically also imperfect. Even marginal mismodeling of the measurement setup is known to ruin the reconstruction of the conductivity in *absolute* EIT [3]. In consequence, it is well motivated to develop algorithms that are robust with respect to (geometric) modeling errors. See [6, 8, 9] for some previous techniques for dealing with uncertainties in the measurement configuration of EIT.

This work employs (stochastic) polynomial collocation for handling absolute EIT imaging with an unknown object shape; consult [7] for more detailed information. The conductivity, the contact resistances, the electrode positions and the exterior boundary of the imaged body are parametrized by a vector whose components live in a bounded interval. The forward problem of the CEM is then considered as a parametric elliptic boundary value problem; the associated solution depends not only on the current feed and the spatial variable but also on the high-dimensional parameter vector. This forward problem is tackled by a (stochastic) collocation finite element method [1]: The CEM problem is first solved with a standard finite element method for the conductivities and measurement settings defined by a sparse grid of Clenshaw–Curtis quadrature points in the parameter hypercube. The dependence of the forward solution on the parameter vector is subsequently generalized to the whole hypercube using collocation by tensor products of Legendre polynomials. This enables simultaneous reconstruction of

all the unknown parameters defining the measurement setup, e.g., by Tikhonov regularization, which leads to minimizing an explicitly known squared multivariate polynomial. The described approach results in a functional reconstruction algorithm that can be applied to both simulated and experimental data; see [7] for the details.

REFERENCES

- [1] I. Babuška, F. Nobile and R. Tempone, *A stochastic collocation method for elliptic partial differential equations with random input data*, SIAM Rev. **52** (2010), 317–355.
- [2] L. Borcea, *Electrical impedance tomography*, Inverse problems **18** (2002), R99–R136.
- [3] W. Breckon and M. Pidcock, *Data errors and reconstruction algorithms in electrical impedance tomography*, Clin. Phys. Physiol. Meas. **9** (1988), 105–109.
- [4] M. Cheney, D. Isaacson and J. Newell, *Electrical impedance tomography* SIAM Rev. **41** (1999), 85–101.
- [5] K.-S. Cheng, D. Isaacson, J. C. Newell and D. G. Gisser, *Electrode models for electric current computed tomography*, IEEE Trans. Biomed. Eng. **36** (1989), 918–924.
- [6] J. Dardé, N. Hyvönen, A. Seppänen and S. Staboulis, *Simultaneous reconstruction of outer boundary shape and admittance distribution in electrical impedance tomography*, SIAM J. Imaging Sci. **6** (2013), 176–198.
- [7] N. Hyvönen, V. Kaarnioja, L. Mustonen and S. Staboulis, *Polynomial collocation for handling an inaccurately known measurement configuration in electrical impedance tomography*, SIAM J. Appl. Math., accepted.
- [8] V. Kolehmainen, M. Lassas and P. Ola, *Inverse conductivity problem with an imperfectly known boundary*, SIAM J. App. Math. **66** (2005), 365–383.
- [9] A. Nissinen, V. Kolehmainen and J. P. Kaipio, *Reconstruction of domain boundary and conductivity in electrical impedance tomography using the approximation error approach*, Int. J. Uncertainty Quantif. **1** (2011), 203–222.
- [10] E. Somersalo, M. Cheney and D. Isaacson, *Existence and uniqueness for electrode models for electric current computed tomography*, SIAM J. Appl. Math. **52** (1992), 1023–1040.
- [11] G. Uhlmann, *Electrical impedance tomography and Calderón’s problem*, Inverse Problems **25** (2009), 123011.

Detecting inclusions within inclusions in electrical impedance tomography

SAMULI SILTANEN

(joint work with Allan Greenleaf, Matti Lassas, Matteo Santacesaria and Gunther Uhlmann)

Electrical impedance tomography (EIT) aims to reconstruct the electric conductivity inside a body from current and voltage measurements at the boundary. In many important applications of EIT the interest is in detecting the location of interfaces between regions of smooth conductivity.

In [5], a method is introduced for recovering singularities in conductivity from EIT measurements. The method is based on a novel use of the so-called *complex geometrical optics* (CGO) solutions introduced by Sylvester and Uhlmann [7], and it is capable of detecting inclusions within inclusions in an unknown inhomogeneous background conductivity. This property is crucial for example in using EIT for

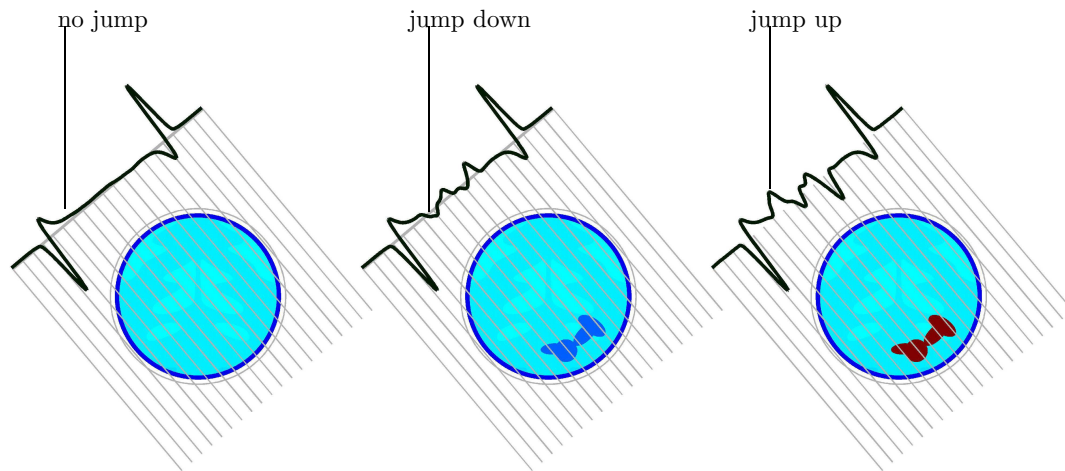


FIGURE 1. Jumps in the conductivity cause signals in the data analogously to parallel-beam X-ray tomography. We illustrate this here using stroke-type phantoms. **Left:** Intact brain. Dark blue ring, with low conductivity, models the skull. **Middle:** Ischemic stroke, or blood clot preventing blood flow to the dark blue area. The conductivity in the affected area is lower than background. **Right:** Hemorrhagic stroke, or bleeding in the brain. The conductivity in the affected area is higher than background. The function shown is $T^{a,+}\mu(t/2, e^{i\varphi}) - T^{a,-}\mu(t/2, e^{i\varphi})$, and φ indicates a direction perpendicular to the virtual “X-rays.”

classifying strokes into ischemic (an embolism preventing blood flow to part of the brain) and hemorrhagic (bleeding in the brain).

EIT can be modeled mathematically using the inverse conductivity problem of Calderón [4]. Consider a bounded, simply connected domain $\Omega \subset \mathbb{R}^2$ with smooth boundary and a scalar conductivity coefficient $\sigma \in L^\infty(\Omega)$ satisfying $\sigma(x) \geq c > 0$ almost everywhere. Applying a voltage distribution f at the boundary leads to the elliptic boundary-value problem

$$(1) \quad \nabla \cdot \sigma \nabla u = 0 \quad \text{in } \Omega, \quad u|_{\partial\Omega} = f.$$

Infinite-precision measurements are modeled by the Dirichlet-to-Neumann map

$$(2) \quad \Lambda_\sigma : f \mapsto \sigma \frac{\partial u}{\partial \vec{n}} \Big|_{\partial\Omega},$$

where \vec{n} is the outward normal vector of $\partial\Omega$.

In [2], the construction of the CGO solutions was done via a Beltrami equation. Identify \mathbb{R}^2 with \mathbb{C} by setting $z = x_1 + ix_2$ and define a Beltrami coefficient,

$$\mu(z) = (1 - \sigma(z))/(1 + \sigma(z)).$$

We have $|\mu(z)| \leq 1 - \epsilon$ for some $\epsilon > 0$. Further, if we assume $\sigma \equiv 1$ outside some $\Omega_0 \subset\subset \Omega$, then $\text{supp}(\mu) \subset \overline{\Omega_0}$. Now consider the unique solution of

$$(3) \quad \bar{\partial}_z f_{\pm}(z, k) = \pm \mu(z) \overline{\partial_z f_{\pm}(z, k)}; \quad e^{-ikz} f_{\pm}(z, k) = 1 + \omega^{\pm}(z, k),$$

where $ikz = ik(x_1 + ix_2)$ and $\omega^{\pm}(z, k) = \mathcal{O}(1/|z|)$ as $|z| \rightarrow \infty$. Here z is a spatial variable and $k \in \mathbb{C}$ a spectral parameter. Also, $u = \text{Re}f_+$ satisfies (1).

The new idea is to apply a partial Fourier transform in the radial direction of k . Write $k = \tau e^{i\varphi}$ and define

$$(4) \quad \widehat{\omega}^{\pm}(z, t, e^{i\varphi}) = \mathcal{F}_{\tau \rightarrow t}(\omega^{\pm}(z, \tau e^{i\varphi})).$$

Recall that the traces of CGO solutions can be recovered perfectly from Λ_{σ} [2, 1] and approximately from practical EIT data [3]. Figure 1 suggests that what we can recover resembles parallel-beam X-ray projection data of the singularities of σ . Indeed, in [5] reconstruction formulae are derived for σ analogous to the classical filtered back-projection method of X-ray tomography.

Formally one can view the Beltrami equation (3) as a scattering equation, where μ is considered as a compactly supported scatterer and the ‘‘incident field’’ is the constant function 1. Consider a ‘‘scattering series’’ for the unaveraged ω^{\pm} ,

$$(5) \quad \omega^{\pm} = \sum_{j=0}^{\infty} \omega_j^{\pm}$$

and set $\widehat{\omega}_j^{\pm} = \mathcal{F}_{\tau \rightarrow t} \omega_j^{\pm}$ as in (4). The derivation of (5) makes use of [6].

Let $X = \{\mu \in L^{\infty}(\Omega); \text{supp}(\mu) \subset \Omega_0, \|\mu\|_{L^{\infty}(\Omega)} \leq 1 - \epsilon\}$, recalling that $\Omega_0 \subset\subset \Omega$. The expansion in (5) comes from the following:

The nonlinear operator $W_k : X \rightarrow L^2(\Omega)$, defined by

$$W_k^{\pm}(\mu) = \omega_{\mu}^{\pm}(\cdot, k)$$

has Fréchet derivatives, denoted by $D^j W_k|_{\mu}$, of all orders $j \in \mathbb{N}$ at $\mu \in X$ and the multiple scattering terms in (5) are given by

$$(6) \quad \omega_j^{\pm} = D^j W_k^{\pm}|_0(\mu, \mu, \dots, \mu).$$

The j -th order scattering operators,

$$(7) \quad T_j^{\pm} : \mu \mapsto \widehat{\omega}_j^{\pm} := \mathcal{F}_{\tau \rightarrow t}(\omega_j^{\pm}(z, \tau e^{i\varphi})), \quad z \in \partial\Omega, t \in \mathbb{R}, e^{i\varphi} \in \mathbb{S}^1,$$

are generalized Fourier integral operators whose wave-front relations can be explicitly computed (see [5]).

Define averaged operators $T_j^{a,\pm}$ for $j = 1, 2, 3, \dots$ and $T^{a,\pm}$ by the complex contour integral,

$$(8) \quad T_j^{a,\pm} \mu(t, e^{i\varphi}) = \frac{1}{2\pi i} \int_{\partial\Omega} \widehat{\omega}_j^{\pm}(z, t, e^{i\varphi}) dz,$$

$$(9) \quad T^{a,\pm} \mu(t, e^{i\varphi}) = \frac{1}{2\pi i} \int_{\partial\Omega} \widehat{\omega}^{\pm}(z, t, e^{i\varphi}) dz,$$

with ω_j^{\pm} defined via formulas (6)–(7) and ω^{\pm} defined via (3). Now $T^{a,\pm}$ are recoverable from EIT data, and one can (to some extent) understand its singularities,

and derive approximate reconstruction formulas, by analyzing the operators $T_j^{a,\pm}$. See [5] for more details.

REFERENCES

- [1] K. ASTALA AND L. PÄIVÄRINTA, *A boundary integral equation for Calderón's inverse conductivity problem*, in Proc. 7th Intern. Conf. on Harmonic Analysis, Collectanea Mathematica, 2006.
- [2] K. ASTALA AND L. PÄIVÄRINTA, *Calderón's inverse conductivity problem in the plane*, Annals of Math., **163** (2006), 265–299.
- [3] K. ASTALA, J. MUELLER, L. PÄIVÄRINTA, A. PERÄMÄKI, AND S. SILTANEN, *Direct electrical impedance tomography for nonsmooth conductivities*, Inverse Probl. Imag., **5** (2011), 531–549.
- [4] A.-P. CALDERÓN, *On an inverse boundary value problem*, in Seminar on Numerical Analysis and its Applications to Continuum Physics (Rio de Janeiro, 1980), Soc. Brasil. Mat., Rio de Janeiro, 1980, 65–73.
- [5] Greenleaf A, Lassas M, Santacesaria M, Siltanen S, Uhlmann G. Propagation and recovery of singularities in the inverse conductivity problem. arXiv preprint arXiv:1610.01721. 2016 Oct 6.
- [6] M. HUHTANEN AND A. PERÄMÄKI, *Numerical solution of the R-linear Beltrami equation*, Math. of Comp., **81** (2012), 387–397.
- [7] J. SYLVESTER AND G. UHLMANN, *A global uniqueness theorem for an inverse boundary value problem*, Ann. of Math. **125** (1987), 153–169.

Stekloff eigenvalues in inverse scattering

DAVID COLTON

We consider a problem in non-destructive testing in which small changes in the (possibly complex valued) refractive index $n(x)$ of an inhomogeneous medium of compact support are to be determined from changes in measured far field data due to incident plane waves. The problem is studied by considering a modified far field operator \mathcal{F} whose kernel is the difference of the measured far field pattern due to the scattering object and the far field pattern of an auxiliary scattering problem with the Stekloff boundary condition imposed on the boundary of a domain B where B is either the support of the scattering object or a ball containing the scattering object in its interior. It is shown that \mathcal{F} can be used to determine the Stekloff eigenvalues corresponding to B where if $B \neq D$ the refractive index is set equal to one in $B \setminus \overline{D}$. A formula is obtained relating changes in $n(x)$ to changes in the Stekloff eigenvalues and numerical examples are given showing the effectiveness of determining changes to the refractive index in this way.

A fast and robust sampling method in inverse acoustic scattering problems

XIAODONG LIU

In the last twenty years, sampling methods for shape reconstruction in inverse scattering problems have attracted a lot of interest. Typical examples include the Linear Sampling Method by Colton and Kirsch [3], the Singular Sources Method by Potthast [11] and the Factorization Method by Kirsch [6]. The basic idea is to design an indicator which is big inside the underlying scatterer and relatively small outside. We refer to the monographs of Cakoni and Colton [1], Colton and Kress [4] and Kirsch and Grinberg [7] for a comprehensive understanding. We also refer to Liu and Zhang [10] for a recent progress on the Factorization Method. Recently, a type of direct sampling methods are proposed for inverse scattering problems, e.g., Orthogonality Sampling by Potthast [12], Direct Sampling Method by Ito et.al. [5], Single-shot Method by Li et.al. [8], Reverse Time Migration by Chen et.al. [2]. These direct sampling methods inherit many advantages of the classical ones, e.g., they are independent of any a priori information on the geometry and physical properties of the unknown objects. The main feature of these direct sampling methods is that only inner product of the measurements with some suitably chosen functions is involved in the computation of the indicator, thus is robust to noises and computationally faster than the classical sampling methods. However, the theoretical foundation of the direct sampling methods is far less well developed than for the classical sampling methods. In particular, there are no theoretical analysis of the indicators for the sampling points inside the scatters.

In this talk, we propose a new direct sampling method for inverse acoustic scattering problems by using the far field measurements. The proposed indicator is given by

$$(1) \quad I_{new}(z) := \left| \int_{S^{n-1}} e^{-ik\hat{\theta}\cdot z} \int_{S^{n-1}} u^\infty(\hat{x}, \hat{\theta}) e^{ik\hat{x}\cdot z} ds(\hat{x}) ds(\hat{\theta}) \right|^\rho, \quad z \in \mathbb{R}^n.$$

In this talk, we showed the following behaviors of the new indicator

- $I_{new}(z)$ has a positive lower bound for each sampling points inside.
- $I_{new}(z) \rightarrow 0$ as $|z| \rightarrow \infty$;
- $I_{new}(z)$ decays like bessel functions as the sampling point z away from the boundary;
- $I_{new}(z)$ is robust to noise.

Here is an example. We choose a kite shaped domain with Dirichlet boundary condition as an unknown object. We set three different wave numbers $k = 5, 10$ and 15 and three different powers $\rho = 1, 2$ and $\rho = 8$. The corresponding observation and incident direction number $N = 16 * k$. The research domain is $[-4, 4] \times [-4, 4]$ with 151×151 equally spaced sampling points. Figure 1 shows the corresponding reconstructions. Obviously, the shadows are greatly reduced with the increase of wave number k and the power ρ . To our surprise, it seems that the indicator always takes its maximum on the boundary of the scatterer, which

results in a sharper reconstruction of the boundary of the scatterer. However, there is no general theory for this fact.

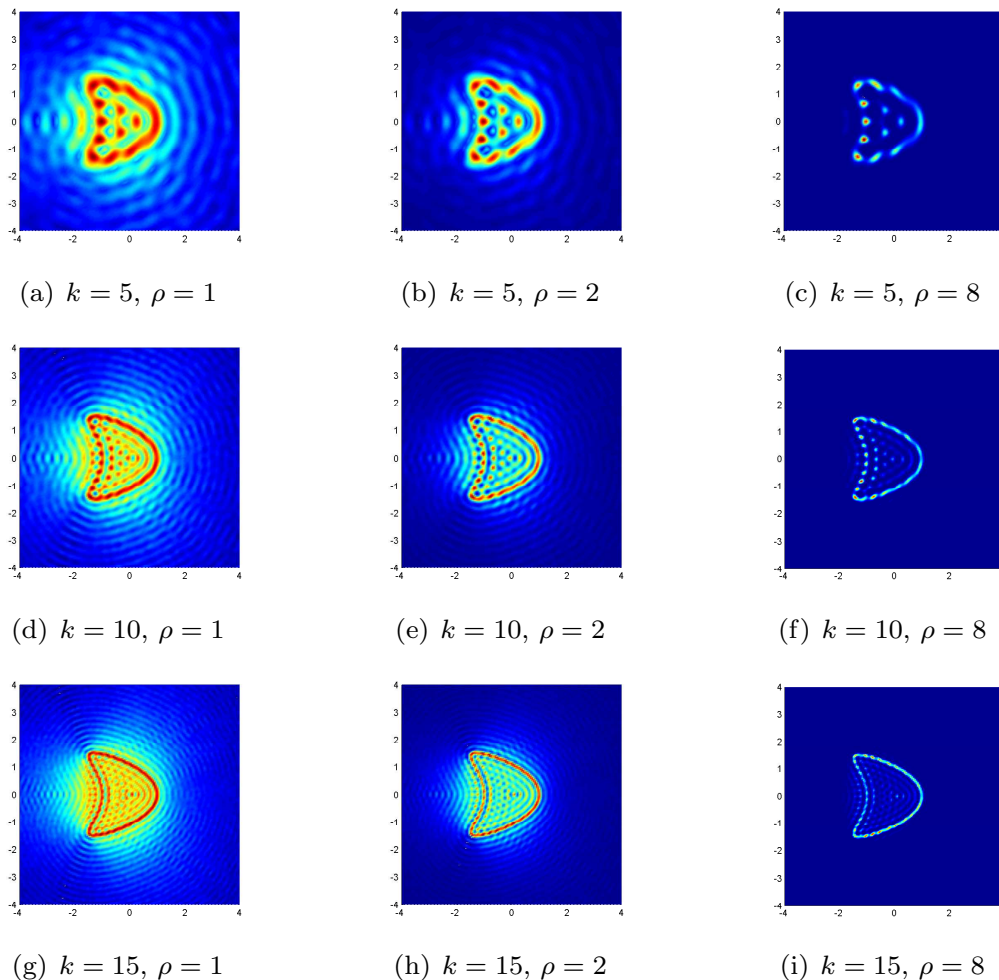


FIGURE 1. **Example HighResolution.** Reconstruction by using different indicators I_{new}^ρ with different wave numbers k and different powers ρ . 30% noise is added to the far field data.

We observe that the reconstructions are rather satisfactory, with the consideration of the severe ill-posedness of the inverse scattering problems and the fact that at least 30% noise is added in the measurements (far field patterns). Actually, the recovering scheme works independently of the physical properties of the underlying scatters. There might be several components with different physical properties, or with different scalar sizes, presented simultaneously. Our method also allows us to distinguish two components of distance about one half of the wavelength, which is known to be challenging for numerical reconstruction. We refer to [9] for more details and numerical examples.

REFERENCES

- [1] F. Cakoni and D. Colton, *A Qualitative Approach in Inverse Scattering Theory*, AMS Vol.188, Springer-Verlag, 2014.
- [2] J. Chen, Z. Chen and G. Huang, Reverse Time Migration for Extended Obstacles: Acoustic Waves, *Inverse Problems* **29**, (2013), 085005.
- [3] D. Colton and A. Kirsch, A simple method for solving inverse scattering problems in the resonance region. *Inverse Problems* **12** (1996), 383–393.
- [4] D. Colton and R. Kress, *Inverse Acoustic and Electromagnetic Scattering Theory* (Third Edition), Springer, 2013.
- [5] K. Ito, B. Jin, and J. Zou, A direct sampling method to an inverse medium scattering problem, *Inverse Problems*, **28**, (2012), 025003.
- [6] A. Kirsch, Characterization of the shape of a scattering obstacle using the spectral data of the far field operator, *Inverse Problems* **14**, (1998), 1489–1512.
- [7] A. Kirsch and N. Grinberg, *The Factorization Method for Inverse Problems*, Oxford University Press, 2008.
- [8] J. Li, H. Liu and J. Zou, Locating multiple multiscale acoustic scatterers, *SIAM Multiscale Model. Simul.*, **12**, (2014), 927–952.
- [9] X. Liu, A fast and robust sampling method for shape reconstruction in inverse acoustic scattering problems, submitted, 2016. Available on <http://www.escience.cn/people/xdliu/index.html>
- [10] X. Liu and B. Zhang, Recent progress on the factorization method for inverse acoustic scattering problems (in Chinese), *Sci Sin Math*, **45**, (2015), 873–890.
- [11] R. Potthast, Stability estimates and reconstructions in inverse acoustic scattering using singular sources, *J. Comput. Appl. Math.*, **114**, (2010), 247–274.
- [12] R. Potthast, A study on orthogonality sampling, *Inverse Problems*, **26**, (2010), 074075.

Halfspace matching for 2D open waveguides

JULIAN OTT

(joint work with A.S. Bonnet-ben-Dhia, S. Fliss, A. Tonnoir, C. Hazard)

We study a numerical method to compute solutions for scattering by a junction of open waveguides in 2D, modeled by the Helmholtz equation with Dirichlet boundary conditions

$$(1) \quad \Delta u(x) + (k^2(x) + i\epsilon)u(x) = 0, \quad x \in \mathbb{R}^2 \setminus \overline{D}, \quad u = f \quad \text{on } \partial D, \quad u \in L^2(\mathbb{R}^2 \setminus \overline{D}),$$

with some limiting absorption $\epsilon > 0$ and space-dependent wavenumber $k : \mathbb{R}^2 \setminus \overline{D} \rightarrow \mathbb{R}$. The wavenumber is assumed to be piecewise constant, with a number of unbounded perturbations, which we will call waveguides (see Figure 1). The interior domain is assumed to be a triangle, but the method works identically if D is a rectangle. We assume that the waveguides are semi-infinite strips, which extend perpendicularly from the sides of the triangle to infinity. The basic idea behind the method is the following: The exterior domain $\mathbb{R}^2 \setminus \overline{D}$ is separated into 3 overlapping halfspaces Ω_n , $n = 1, 2, 3$, with boundaries $\Gamma_n = \Gamma_n^+ \cup \Gamma_n^0 \cup \Gamma_n^-$. The method now exploits that given some Dirichlet data $u^{(0)} \in H^{1/2}(\mathbb{R})$, the Dirichlet *halfspace problem* of finding a solution $u : \mathbb{R} \times (0, \infty) \rightarrow \mathbb{C}$ to

$$\Delta u(x) + (k^2(x_1) + i\epsilon)u(x) = 0, \quad x \in \mathbb{R} \times (0, \infty), \quad u(x_1, 0) = u^{(0)}(x_1) \quad x_1 \in \mathbb{R},$$

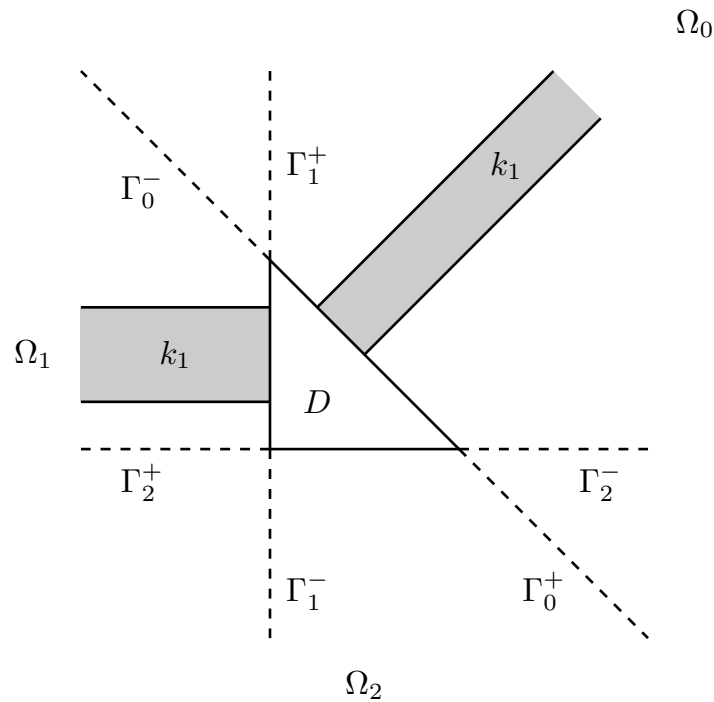


FIGURE 1. Illustration of the geometry and notation: The exterior of the triangle D is separated in 3 overlapping halfspaces Ω_n , $n \in \{0, 1, 2\}$. The wavenumber $k(x)$ is equal to k_1 inside the grey areas, and equal to k_0 outside.

allows an explicit representation with the help of the spectral family of $A = \frac{\partial^2}{\partial x_1^2} + k^2(x_1)$. Namely,

$$(2) \quad \begin{aligned} u(x) = & \sum_{n=1}^N e^{-\sqrt{\lambda_n - k_0^2 - i\epsilon} x_2} \phi_n(x_1) \langle u^{(0)}, \phi_n \rangle_{L^2(\mathbb{R})} \\ & + \frac{1}{2\pi} \sum_{\nu \in \{+, -\}} \int_{\mathbb{R}} e^{-\sqrt{\lambda - k_0^2 - i\epsilon} x_2} \psi_\lambda^\nu(x_1) \langle u^{(0)}, \psi_\lambda^\nu \rangle_{L^2(\mathbb{R})} d\lambda. \end{aligned}$$

The functions $\phi_n : \mathbb{R} \rightarrow \mathbb{C}$ are $L^2(\mathbb{R})$ eigenfunctions of A , while for $\lambda \in \mathbb{R}$ the functions $\psi_\lambda^\pm : \mathbb{R} \rightarrow \mathbb{C}$ are so called generalized eigenfunctions of A : The eigenfunctions and generalized eigenfunctions can be computed explicitly for simple forms of k . In particular for the case $k(x_1) = k_1$ if $x_1 \in (-h, h)$, and $k(x_1) = k_0$ else, they are readily available from literature (see [1, 2]). If $k_1 > k_0$, there is a finite number of eigenfunctions of A , whose corresponding terms under the finite sum in (2) are called “modes” of the open waveguide.

Going back to the exterior problem in $\mathbb{R}^2 \setminus \overline{D}$, the basic idea of the *Halfspace matching* method is the following: If we know the traces

$$u_n^\nu := u|_{\Gamma_n^\nu}, \quad \nu \in \{+, -\}, n \in \{0, 1, 2\},$$

we can reconstruct the solution of (1) with the help of (2), applied to the different halfspaces Ω_n , $n \in \{1, 2, 3\}$. Hence, let us denote by $S_n : H^{1/2}(\Gamma_n) \rightarrow H^1(\Omega_n)$

the Halfspace solution operators, which map some Dirichlet data from $H^{1/2}(\Gamma_n)$ to the solution on the Halfspace Ω_n . Then, by considering a solution u of (1), we obtain that it's traces must fulfill

$$(3) \quad u_n^\pm = (S_n(u_n^+ + u_n^0 + u_n^-))|_{\Gamma_{n\pm 1}^\pm}, \quad n \in \mathbb{Z}/3\mathbb{Z}.$$

Let us comment a bit further on the last set of equations: It contains 6 unknowns, the traces of the on the semi-infinity boundaries Γ_n^+, Γ_n^- , while the traces on the bounded parts Γ_n^0 are known. It is also a set of 6 equations, for each halfspace $n \in \{1, 2, 3\}$ and each direction $\pm = +$ and $\pm = -$. Our main result is the following:

Theorem. *The compatibility equations (3) are Fredholm in $L^2(\Gamma_0^+) \times L^2(\Gamma_0^-) \times \dots \times L^2(\Gamma_2^-)$ with trivial Kernel.*

Hence we can solve the compatibility equations (3) instead of the original problem (1). This effectively reduces the dimension of the problem by one, and can be coupled with a finite element method inside the bounded triangle D to numerically approximate solutions on the whole of \mathbb{R}^2 . Numerical examples and some applications were presented, where this method has been used to solve some scattering problem.

This type of method has already been applied to different types of problem, see [3, 4].

REFERENCES

- [1] C.H. Wilcox, *Sound propagation in stratified fluids*, Applied Mathematical Sciences **50**, Springer (1984).
- [2] R. Magnanini and F. Santosa, *Wave propagation in a 2-D optical waveguide*, SIAM J. Appl. Math **61** (2000/01), no. 4, 1237–1252.
- [3] C. Besse, J. Coatléven, S. Fliss, I. Lacroix-Violet, K. Ramdani, *Transparent boundary conditions for locally perturbed infinite hexagonal periodic media*, Commun. Math. Sci. **11** (2013), no. 4, 907–938.
- [4] A. Tonnoir, *Conditions transparentes pour la diffraction d'ondes en milieu élastique anisotrope*, PhD Thesis, ENSTA ParisTech, 2015.

Analysis of electromagnetic waves in random media

LILIANA BORCEA

(joint work with Josselin Garnier)

The understanding of the interaction of electromagnetic waves with heterogeneous media with small microstructure is of great important in applications like polarimetric radar imaging, specially in high frequency regimes like X-band, where the waves are affected by atmospheric turbulence. We present an analysis of such an interaction using Maxwell's equations in random media with small fluctuations of the electric permittivity. We consider a setup where the waves propagate toward a preferred direction, in a beam-like manner. We decompose the electromagnetic wave field in transverse electric and transverse magnetic plane waves, called modes,

with random amplitudes that model cumulative scattering effects in the medium. Their evolution is described by a coupled system of stochastic differential equations driven by the random fluctuations of the electric permittivity. We analyze the solution of this system with the Markov limit theorem and obtain a detailed asymptotic characterization of the electromagnetic wave field. The asymptotic small parameter is defined by the ratio of the wavelength to the distance of propagation, and scales the standard deviation of the random fluctuations of the electric permittivity. We consider a scaling where these fluctuations cause a significant net scattering effect on the electromagnetic waves. This effect is quantified by a detailed characterization of the loss of coherence of the waves and of the energy exchange between the wave modes. This energy exchange allows us to model the loss of polarization of the waves induced by scattering. It is described mathematically by a transport equation satisfied by the Wigner transform (energy density) of the electromagnetic wave field. This equation is a simplified version of Chandrasekar's transport equations that so far do not have a rigorous mathematical derivation. A main result of our study is the derivation of these equations in a forward scattering regime. We also connect the results with the existing literature in radiative transport and paraxial wave propagation.

Measuring electromagnetic chirality

TILO ARENS

(joint work with Felix Hagemann and Frank Hettlich)

An optically active material will produce a response to an electromagnetic wave propagating through it that depends on the circular polarization state of the wave, i.e. on its *helicity*. On the other hand, chirality may also be caused simply by the geometry of an individual scatterer. Recently, a novel definition of chirality was proposed in the Physics literature [1] for scattering of electromagnetic waves that includes both aspects and moreover allows to measure *how chiral* a given scatterer is. We will discuss this definition and some of its consequences in the mathematical framework of time-harmonic wave propagation and incident Herglotz wave pairs.

A Herglotz wave pair $(E, H) = \int_{\mathbb{S}^2} (A(d), d \times A(d)) e^{i k d \cdot x} ds(d)$ is characterized by its amplitude density $A \in L_t^2(\mathbb{S}^2)$. Circularly polarized Herglotz wave functions (i.e. fields of one helicity) can be characterized as eigenfunctions for the eigenvalues ± 1 of the operator $\mathcal{C} : A \mapsto i d \times A(d)$ in $L_t^2(\mathbb{S}^2)$. This space is hence seen to be the direct sum of the corresponding orthogonal eigenspaces $L_t^2(\mathbb{S}^2) = V^+ \oplus V^-$.

A scattering problem in this framework is fully described by the *far field operator* $\mathcal{F} : L_t^2(\mathbb{S}^2) \rightarrow L_t^2(\mathbb{S}^2)$ mapping the amplitude function to the far field pattern of the scattered electric field. Using the orthogonal projections \mathcal{P}^\pm onto V^\pm , contributions due to different helicities can be identified by setting

$$\mathcal{F}^{pq} = \mathcal{P}^p \mathcal{F} \mathcal{P}^q, \quad p, q \in \{+, -\}.$$

Hence $\mathcal{F} = \sum_{p, q \in \{+, -\}} \mathcal{F}^{pq}$. Translating the definition in [1] into this framework yields the following

Definition The scatterer D is called *electromagnetically achiral* (*em-achiral*) if there exist unitary operators $\mathcal{U}^{(j)}$ in $L_t^2(\mathbb{S}^2)$ with $\mathcal{U}^{(j)}\mathcal{C} = -\mathcal{C}\mathcal{U}^{(j)}$, $j = 1, \dots, 4$, such that

$$\mathcal{F}^{++} = \mathcal{U}^{(1)}\mathcal{F}^{--}\mathcal{U}^{(2)}, \quad \mathcal{F}^{-+} = \mathcal{U}^{(3)}\mathcal{F}^{+-}\mathcal{U}^{(4)}.$$

If this is not the case, we call the scatterer D *em-chiral*.

We show, firstly, that for the standard problems of scattering by a perfect conductor or for a transmission problem for a bounded scatterer with constant material properties, geometric achirality also implies em-achirality. Here, geometric achirality means that the scatterer can be mapped onto itself by an affine transform with an orthogonal matrix with determinant -1 .

Secondly, following the idea in [1], a *measure of chirality* can be defined via singular systems for the operators \mathcal{F}^{pq} . Denoting by $(\sigma_j^{pq}, G_j^{pq}, H_j^{pq})$ a singular system of \mathcal{F}^{pq} for a scatterer D , we set

$$\chi(\mathcal{F}) = (\|(\sigma_j^{++}) - (\sigma_j^{--})\|_{\ell^2}^2 + \|(\sigma_j^{+-}) - (\sigma_j^{-+})\|_{\ell^2}^2)^{1/2}.$$

Also using a singular system (σ_j, G_j, H_j) for \mathcal{F} , define the *total interaction cross section* of D by $C_{\text{int}}(\mathcal{F}) = \sum_j \sigma_j^2$. It can be shown, that if a scatterer is invisible to fields of one helicity, then it has maximum measure of chirality among all scatterers of the same total interaction cross section. The reverse also holds true if a reciprocity relation is fulfilled for the scattering problem under consideration.

Lastly, using results from [2], it can be shown that a scattering problem for a ball made of a chiral material in the sense of the Drude-Born-Fedorov model, leads to an em-chiral scatterer in the sense of the above definition. Hence the definition indeed captures the complete range of chirality for electromagnetic wave scattering problems.

Future research will be aimed at getting an improved understanding of this notion of chirality. In particular, the proposed measure of chirality is to be used to obtain scatterers close to invisible to one helicity by using shape optimization techniques.

REFERENCES

- [1] I. Fernandez-Corbaton, M. Fruhnert and C. Rockstuhl, *Objects of maximum electromagnetic chirality*, Phys. Rev. X **6** (2016), 031013, doi: 10.1103/PhysRevX.6.031013.
- [2] S. Heumann, *The Factorization Method for Inverse Scattering from Chiral Media*, PhD thesis, Karlsruhe Institute of Technology, 2012.

The inverse electromagnetic scattering problem in OCT for anisotropic media

OTMAR SCHERZER

(joint work with Peter Elbau, Leonidas Mindrinos)

In this work we consider the inverse electromagnetic scattering problem for inhomogeneous anisotropic media placed in an Optical Coherence Tomography (OCT) system.

OCT is a non-invasive imaging technique producing high-resolution images of biological tissues. It is based on low (time) coherence interferometry and it is capable of imaging micro-structures within a few micrometers resolution. Standard OCT operates using broadband and continuous wave light in the visible and near-infrared spectrum. Images are obtained by measuring the time delay and the intensity of back-scattered light from the sample under investigation. There also exist contrast-enhanced OCT techniques like polarisation-sensitive OCT (PS-OCT) which allows for simultaneously detecting different polarisation states of the back-scattered light [2].

We model the propagation of electromagnetic waves through the inhomogeneous anisotropic medium using Maxwell's equations [1]. The sample is hereby considered as a linear dielectric non-magnetic medium. Moreover, we assume that it is weakly scattering, meaning that the electromagnetic field inside the medium is sufficiently well described by a first order Born approximation.

The optical properties of the medium are then characterised by the electric susceptibility $\chi : \mathbb{R} \times \mathbb{R}^3 \rightarrow \mathbb{R}^{3 \times 3}$, the quantity to be recovered, where the causality requires that $\chi(t, x) = 0$ for $t < 0$. The measurements M are given as a combination of the back-scattered field by the sample and the back-reflected field from a reference mirror. In an OCT system, the detector is placed in a distance much bigger than the size of the medium, therefore we consider as measurement data the far field approximation of the electromagnetic field.

Then, the direct problem is modelled as an integral operator \mathcal{F} mapping the susceptibility χ to the measurement data M . The inverse problem we are interested in is to solve the operator equation

$$\mathcal{F}\chi = M$$

for χ , given measurements for different positions of the mirror and different incident polarisation vectors. Under some restrictions on the OCT setup [3] and assuming that the incoming plane wave $E^{(0)}$ propagates in the direction $-e_3$, we can formulate the inverse problem as the reconstruction of χ from the expressions

$$(1) \quad \mathcal{H}_j^{-1}M = p_j[\vartheta \times (\vartheta \times \tilde{\chi}(\omega, \frac{\omega}{c}(\vartheta + e_3))p)]_j, \quad j = 1, 2,$$

where \mathcal{H}_j are some explicitly known, well-posed operators, $p \in \mathbb{R}^2 \times \{0\}$ is the polarisation of the initial illumination, $\omega \in \mathbb{R} \setminus \{0\}$ is the frequency and $\vartheta \in S_+^2$ is the direction from the origin (where the sample is located) to a detector point. Here $\tilde{\chi}$ denotes the Fourier transform of χ with respect to time and space.

In the special case of an isotropic medium, meaning that χ is a multiple of the unit matrix, it remains the problem to reconstruct the four dimensional susceptibility from the three dimensional measurement data. We propose an iterative scheme, assuming a certain discretisation of χ with respect to the detection points and its support, that provides us with the values of a limited angle Radon transform. For non-dispersive media, where the temporal Fourier transform $\hat{\chi}$ of χ does not depend on frequency, the equation (1) determines the spatial Fourier

transform of $\hat{\chi}$ in a cone. Thus, the problem reduces to the inversion of the three-dimensional Fourier transform with limited data and there exist several algorithms for recovering the scalar susceptibility under these assumptions.

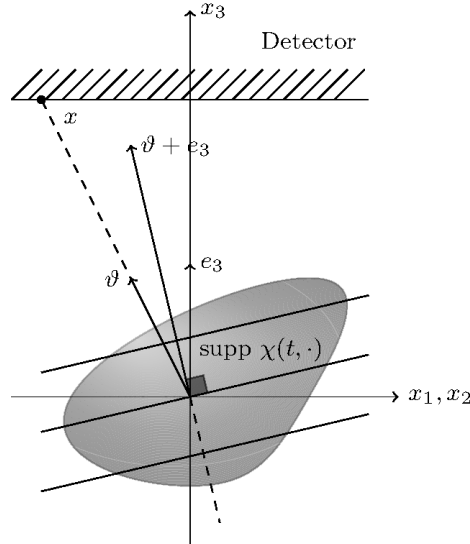


FIGURE 1

For the most general case of a matrix valued susceptibility (non-symmetric), using the discretisation of χ we show that three incident polarisation vectors uniquely determine the Radon transform of the projection of χ over planes orthogonal to the vector $\vartheta + e_3$, see Figure 1. To be able to recover the Fourier transform of χ we have to repeat the experiment for different orientations of the sample. More precisely, we have to tilt slightly the sample three times for every incident polarisation.

The above analysis concerns the study of standard OCT where the sample is illuminated by light with fixed polarisation (usually linear).

On the other hand, in PS-OCT the interferometer with the addition of polarizers and quarter-wave plates change the polarisation state of light to produce circularly polarized light incident on the sample. The output signal now is split into its horizontal and vertical components to be measured at two different photo detectors. In this setting, we consider an orthotropic non-dispersive medium where the susceptibility is now a symmetric matrix with only four unknowns and its temporal Fourier transform is frequency independent.

From [1] we know that the scattered field can be written as a linear integral operator \mathcal{G} applied to the product of the temporal Fourier transforms $\hat{\chi}$ and $\hat{E}^{(0)}$ of the susceptibility χ and the incident field $E^{(0)}$, respectively. The kernel of the operator \mathcal{G} is the Green tensor related to Maxwell's equations in the frequency domain. This relation is known as Lippmann–Schwinger equation. The k th order Born approximation $\hat{E}^{(k)}$ is defined by

$$\hat{E}^{(k)} = \hat{E}^{(0)} + \mathcal{G}[\hat{\chi}\hat{E}^{(k-1)}], \quad k \in \mathbb{N}.$$

We consider the second order Born approximation together with the far field approximation, that affects only the Green tensor resulting to an operator \mathcal{G}^∞ , which

leads to

$$\hat{E}^{(2)} = \hat{E}^{(0)} + \mathcal{G}^\infty[\hat{\chi}(\hat{E}^{(0)} + \mathcal{G}[\hat{\chi}\hat{E}^{(0)}])].$$

We assume that the variations of $\hat{\chi}$ are small compared to the constant background value $\hat{\chi}_0$ (which is given), meaning $\hat{\chi} = \hat{\chi}_0 + \epsilon\hat{\chi}_1$, for some small $\epsilon > 0$. Equating the first order terms we consider only the term

$$\mathcal{G}^\infty[\hat{\chi}_1(\hat{E}^{(0)} + \mathcal{G}[\hat{\chi}_0\hat{E}^{(0)}])] + \mathcal{G}^\infty[\hat{\chi}_0\mathcal{G}[\hat{\chi}_1\hat{E}^{(0)}]]$$

as the one that has the necessary information. Similar to the derivation of (1), the inverse problem of determining $\hat{\chi}_1$ from the OCT measurements, related to the field $\hat{E}^{(2)}$, reduces to the reconstruction of $\hat{\chi}_1$ from the expressions

$$(2) \quad p_j^r [\vartheta \times (\vartheta \times ((\tilde{\chi}_1 + \hat{\chi}_0\mathcal{K}[\tilde{\chi}_1] + \mathcal{L}[\tilde{\chi}_1]\hat{\chi}_0)p^s))]_j, \quad j = 1, 2,$$

for some integral operators \mathcal{K} and \mathcal{L} related to \mathcal{G} and polarisation vectors p^r and p^s describing the change of the polarisation state of light travelling in the reference and sample arm, respectively. These changes can be easily modelled using Jones matrices.

We show that two linear independent incident polarisations provide enough information for recovering $\hat{\chi}_1$. Expression (2), for two incident polarisations of the form $p = e_1$ and $p = e_2$ results in a system of Fredholm integral equations of the second kind for the three (out of four) unknown components of $\hat{\chi}_1$. In addition, the integral operator is compact. The fourth component is given as a solution of a Fredholm integral equation of the first kind, where the right-hand side depends on the three previously computed solutions.

As a future work we plan to consider the numerical implementation of the above results for simulated and real data. Even though we have a theoretical result that makes the reconstruction of $\tilde{\chi}$ possible, we still have to tackle the ill-posedness of the inverse problem. Recall that in a real world experiment we only have access to noisy band-limited and limited-angle measurements due to the limited spectrum of the light source and the size of the detector.

REFERENCES

- [1] D. Colton and R. Kress. Inverse acoustic and electromagnetic scattering theory, volume 93 of Applied Mathematical Sciences. 3rd ed., Springer-Verlag, New York, 2013.
- [2] W. Drexler and J. G. Fujimoto. Optical Coherence Tomography: Technology and Applications. 2nd ed., Springer International Publishing, Switzerland, 2015.
- [3] P. Elbau, L. Mindrinos and O. Scherzer. *Mathematical Methods of Optical Coherence Tomography*. In Handbook of Mathematical Methods in Imaging, Springer, New York, 1169–1204, 2015.

Parameter identification for complex materials using transmission eigenvalues

ISAAC HARRIS

(joint work with Fioralba Cakoni, Housseem Haddar and Shari Moskow)

1. HOMOGENIZATION OF THE TRANSMISSION EIGENVALUES

The first problem that we consider is the transmission eigenvalue problem associated with a highly oscillating anisotropic and/or isotropic periodic media in the frequency domain. This problem is derived from the time-harmonic wave propagation with rapidly oscillating periodic coefficients which is typically associated with materials containing a fine micro-structure. Such composite materials are at the foundation of many modern engineering designs and are used to produce materials with special properties by combining different materials in periodic patterns. In practice, it is desirable to understand the macro-structure (large scale) behavior of the composite materials which mathematically is achievable by using Homogenization Theory [1], [2]. Here we are concerned with the real transmission eigenvalues, in particular their behavior as the period in the medium approaches zero. Transmission eigenvalue problems are a new class of eigenvalue problems that are nonlinear and non self-adjoint which are not covered by standard theory. Such eigenvalues can be determined from the scattering data [3], [4] and provide information about material properties of the scattering media [5], and hence can be used to estimate the effective material properties of the media.

Now let $D \subset \mathbb{R}^m$ where $m = 2, 3$ be a bounded simply connected open set with piecewise smooth boundary ∂D representing the support of the inhomogeneous periodic media. We are interested in the limiting case as $\varepsilon \rightarrow 0$ for the transmission eigenvalue problem given by: find non-trivial $k_\varepsilon \in \mathbb{R}^+$ and $(w_\varepsilon, v_\varepsilon)$ such that

$$(1) \quad \nabla \cdot A(x/\varepsilon)\nabla w_\varepsilon + k_\varepsilon^2 n(x/\varepsilon)w_\varepsilon = 0 \quad \text{and} \quad \Delta v_\varepsilon + k_\varepsilon^2 v_\varepsilon = 0 \quad \text{in } D$$

$$(2) \quad w_\varepsilon = v_\varepsilon \quad \text{and} \quad \frac{\partial w_\varepsilon}{\partial \nu_A} = \frac{\partial v_\varepsilon}{\partial \nu} \quad \text{on } \partial D.$$

Note that the spaces for the solution $(w_\varepsilon, v_\varepsilon)$ will become precise later since they depend on whether $A = I$ or $A \neq I$. We assume that the matrix $A(y) \in L^\infty(Y, \mathbb{R}^{m \times m})$ is Y -periodic symmetric positive definite and the function $n(y) \in L^\infty(Y)$ is a positive Y -periodic function. It is known that as $\varepsilon \rightarrow 0$

$$n(x/\varepsilon) \rightarrow n_h = \frac{1}{|Y|} \int_Y n(y) dy \quad \text{weakly in } L^\infty \quad \text{and}$$

$$A(x/\varepsilon) \rightarrow A_h \quad \text{in the sense of H-convergence.}$$

H-convergence is defined as: given $u_\varepsilon \xrightarrow{w} u$ in $H^1(D)$ then $A(x/\varepsilon)\nabla u_\varepsilon \xrightarrow{w} A_h \nabla u$ in $[L^2(D)]^m$. It can be shown that A_h is a constant symmetric positive definite matrix. In [6] the following results are proven for an infinite set of eigenvalues.

Convergence Result 1: Assume $A = I$ and that $n(y) > 1$ or $n(y) < 1$, then there is a subsequence of $\{k_\varepsilon, (w_\varepsilon, v_\varepsilon)\} \in \mathbb{R}^+ \times L^2(D) \times L^2(D)$ satisfying $(w_\varepsilon, v_\varepsilon)$ converges weakly to $(v, w) \in L^2(D) \times L^2(D)$ and $k_\varepsilon \rightarrow k$ such that

$$\begin{aligned} \Delta w + k^2 n_h w &= 0 \quad \text{and} \quad \Delta v + k^2 v = 0 \quad \text{in} \quad D \\ w &= v \quad \text{and} \quad \frac{\partial w}{\partial \nu} = \frac{\partial v}{\partial \nu} \quad \text{on} \quad \partial D. \end{aligned}$$

Convergence Result 2: Assume that $A(y) - I$ and $n(y) - 1$ have different sign in Y , or $n(y) = 1$ and $A(y) - I$ is positive (or negative) definite. Then there is a subsequence of $\{k_\varepsilon, (w_\varepsilon, v_\varepsilon)\} \in \mathbb{R}^+ \times H^1(D) \times H^1(D)$ satisfying $(w_\varepsilon, v_\varepsilon)$ converges weakly to $(w, v) \in H^1(D) \times H^1(D)$ and $k_\varepsilon \rightarrow k$ that satisfies

$$\begin{aligned} \nabla \cdot A_h \nabla w + k^2 n_h w &= 0 \quad \text{and} \quad \Delta v + k^2 v = 0 \quad \text{in} \quad D \\ w &= v \quad \text{and} \quad \frac{\partial w}{\partial \nu_{A_h}} = \frac{\partial v}{\partial \nu} \quad \text{on} \quad \partial D. \end{aligned}$$

We then give some numerical examples of determining the real transmission eigenvalues from the far field scattering data, then we conclude with some examples demonstrating that the first real transmission eigenvalue provides information about the effective material properties A_h and n_h of the periodic media.

Open Problem: Determining the corrector term in the asymptotic expansion for transmission eigenvalues.

2. ASYMPTOTIC EXPANSION FOR SMALL DEFECTS

Next, we consider the scattering by an anisotropic material with small volume penetrable defects. The goal is to determine how the presence of these defects affects the transmission eigenvalues. Just as in [7], we wish to provide an asymptotic expansion valid for small defects by computing the first order correction term using the analysis in [8]. In the previous section we see that the leading order term (limiting value as $\varepsilon \rightarrow 0$) can be used to determine information about the macro-structure. Therefore, if we want to determine the micro-structure behavior (i.e. coefficients in the defects) we need the correction formula. Having measured transmission eigenvalues from the scattering data one can consider the inverse spectral problem of determining the material properties of the defects using the correction formula.

The time harmonic scattering problem for materials with small volume defects is analogous to the scattering problem in the previous section and we can therefore derive the transmission eigenvalue problem for the perturbed coefficients. The defective regions are denoted by $D_\varepsilon = \bigcup_{m=1}^M (z_m + \varepsilon B_m)$ a subset of D where $\text{dist}(D_\varepsilon, \partial D) \geq c_0 > 0$ and we let the perturbed coefficients be given by

$$A_\varepsilon(x) = A(x)(1 - \chi_{D_\varepsilon}) + \sum_{m=1}^M A_m \chi_{(z_m + \varepsilon B_m)}$$

and

$$n_\varepsilon(x) = n(x)(1 - \chi_{D_\varepsilon}) + \sum_{m=1}^M n_m \chi_{(z_m + \varepsilon B_m)}.$$

The transmission eigenvalue problem for a material with small defects is given by (1)-(2) with the perturbed coefficients A_ε and n_ε . We show that the transmission eigenvalues of the perturbed media converge to the transmission eigenvalues of the unperturbed media as $\varepsilon \rightarrow 0$. Then, we derive the correction formula for simple eigenvalues with $n_m = n$, which contain the matrix contrast in the defect $A_m - A$ and a polarization constant (see [9] for details). Some technical limitations of our analysis:

Open Problems:

- $A - I$ and $A_m - I$ must both be positive (or negative definite)
- The asymptotic formula is only valid for simple eigenvalues
- The asymptotic formula is only valid when $n = n_m$

This is forthcoming work:

F. Cakoni, I. Harris and S. Moskow, "The MUSIC algorithm and perturbation of the transmission eigenvalues for an anisotropic media in the presence of small inhomogeneities. *Under Preparation-Working Title*.

REFERENCES

- [1] Allaire G, *Shape Optimization by the Homogenization Method*, Springer, New York, 2002.
- [2] Bensoussan A, Lions JL and Papanicolaou G, *Asymptotic Analysis for Periodic Structures*, AMS Chelsea Publishing, Providence, 1978.
- [3] Cakoni F, Colton D and Haddar H, "On the determination of Dirichlet or transmission eigenvalues from far field data". *C. R. Math. Acad. Sci. Paris, Ser I*, **348**(7-8): 379–383 (2010).
- [4] A. Lechleiter, S. Peters, "Determining transmission eigenvalues of anisotropic inhomogeneous media from far field data". *Communications in Mathematical Sciences* **13**(7) (2015) 1803–1827.
- [5] Cakoni F, Gintides D and Haddar H, "The existence of an infinite discrete set of transmission eigenvalues" *SIAM J. Math. Anal.* **42**, (2010) 237–255.
- [6] F. Cakoni, H. Haddar, and I. Harris, "Homogenization of the transmission eigenvalue problem for periodic media and application to the inverse problem". *Inverse Problems and Imaging* **9**, No. 4, (2015), 1025–1049
- [7] F. Cakoni, S. Moskow and S. Rome "Perturbations of transmission eigenvalues for inhomogeneous media in the presence of small inclusions". *Inverse Problems and Imaging*, **9**, No. 3, (2015) 725–748.
- [8] S. Moskow, "Nonlinear eigenvalue approximation for compact operators". *Journal of Mathematical Physics* **56** (2015) 113512.
- [9] I. Harris, "Non-Destructive Testing of Anisotropic Materials". *University of Delaware*, Ph.D. Thesis (2015)

The Bloch transform and scattering from locally perturbed periodic structures

ARMIN LECHLEITER

(joint work with Ruming Zhang)

Rather complex micro- or nano-structured dielectric structures become more and more important for modern industrial products involving physical sensors, optical components, or surface coatings. Non-destructive testing of these thin layers via scattered incident electromagnetic waves is a promising way towards fast in-process testing of such structures. As a first step towards a mathematical model for the corresponding scattering process, we consider in this abstract scattering from a locally perturbed periodic structure. This is intended as a first step towards the full electromagnetic scattering problem from a basically random structure, given that today's state of the art of periodic scattering theory is still linked almost exclusively to perfectly periodic settings. More precisely, for a periodic background setting, our theory allows non-periodicity locally in the material parameters and/or in the incident field illuminating the structure.

To simplify presentation, we restrict ourselves to scattering from a surface given as graph of a C^2 -smooth function with Dirichlet boundary conditions in two dimensions. (But note that other scenarios can be treated as well, see [6, 5, 7, 8].) Considering first arbitrary Lipschitz continuous surfaces $\Gamma = \{x_2 = \zeta(x_1)\}$ given by a Lipschitz continuous function $\zeta : \mathbb{R} \rightarrow \mathbb{R}$ that takes values in a bounded interval $(0, H)$, the domain above Γ is $\Omega = \{x_2 > \zeta(x_1)\}$ and $\Omega_H = \{\zeta(x_1) < x_2 < H\}$. Recall the weighted Sobolev spaces

$$\|u\|_{H_r^s(\Omega_H)} = \left\| (x_1, x_2) \mapsto (1 + |x_1|^2)^{r/2} u(x_1, x_2) \right\|_{H^s(\Omega_H)}, \quad s, r \in \mathbb{R}$$

that are defined via the well-known Sobolev spaces $H^s(\Omega_H)$ and polynomial weight functions. Then [1] states that for incident fields u^i that belong to $H_r^1(\Omega_H)$ for some $r \in (-1, 1)$ and solve the Helmholtz equation $\Delta u^i + k^2 u^i = 0$ in the weak sense in Ω , there exists a unique total field $u \in H_r^1(\Omega_H)$ that solves the following surface scattering problem: First, u is a weak solution to the Helmholtz equation that vanishes on Γ , and second the scattered field $u^s := u - u^i$ is upwards radiating. The latter condition is either formulated via the upwards radiation condition or, more typical in our context, via the angular spectrum condition; the latter conditions allow to extend u^s (or u) to all of Ω as a solution to the Helmholtz equation.

We next consider the setting where Γ is a periodic surface defined via a 2π -periodic surface $\zeta \in C^2(\mathbb{R})$ that is locally perturbed in one periodicity cell: For $\zeta_p \in C^2(\mathbb{R})$ such that $\zeta_p(x_1) = \zeta(x_1)$ for $|x_1| \geq \pi$ and $0 < \zeta_p(x_1) < H$ for all $x_1 \in \mathbb{R}$, the perturbed domain is $\Omega_p = \{x_2 > \zeta_p(x_1)\}$ and $\Omega_H^p = \{\zeta_p(x_1) < x_2 < H\}$. Set, additionally, $Q_H^{2\pi} = \{x \in \Omega_H : -\pi < x_1 < \pi\}$ to be the unit cell of the 2π -periodic strip Ω_H and consider a C^1 -diffeomorphism Φ_p between Ω_H and Ω_H^p , such that Φ_p equals the identity in $\Omega_H \setminus Q_H^{2\pi}$, for some $H' < H$.

Rephrasing the above scattering problem via Φ_p one finds that the transformed solution $u_T = u \circ \Phi_p \in H_r^1(\Omega_H)$ satisfies

$$\operatorname{div}(A_p \nabla u_T) + k^2 c_p u_T = 0,$$

subject to Dirichlet boundary conditions on the periodic surface Γ and a radiation condition for the corresponding scattered field. The coefficients A_p and c_p equal the unit matrix and one outside of $Q_H^{2\pi}$, such that this problem can be reformulated on a bounded domain by the (Floquet-)Bloch transform as we sketch next. (See [2, 3, 4] for motivation and alternatives for our approach.)

The Bloch transform \mathcal{J} is defined in the above spaces $H_r^s(\Omega_H)$ by density of $C_0^\infty(\Omega_H)$ as

$$\mathcal{J}u(\alpha, x) = \sum_{j \in \mathbb{Z}} u(x_1 + 2\pi j, x_2) e^{2\pi i j \alpha}, \quad \alpha \in \mathbb{R}, x \in \Omega_H.$$

Apparently, $\mathcal{J}u$ is one-periodic in α and α -quasiperiodic with period 2π in x_1 , that is,

$$\mathcal{J}u(\alpha, (x_1 + 2\pi, x_2)) = e^{-2\pi i \alpha} \mathcal{J}u(\alpha, x), \quad \alpha \in \mathbb{R}, x \in \Omega_H.$$

such that we merely need to consider $\mathcal{J}u$ as a (quasi-)periodic function in α and x . Let us now denote the space of α -quasiperiodic functions in $H_{\text{loc}}^1(\Omega_H)$ by $H_\alpha^1(Q_H^{2\pi})$. Then one can show as in [5] that \mathcal{J} is an isomorphism between $H_r^s(\Omega_H)$ and the Sobolev space $H_{\text{per}}^r((-1/2, 1/2]; H_\alpha^s(Q_H^{2\pi}))$, that the inverse of \mathcal{J} equals

$$\mathcal{J}^{-1}w \left(\begin{matrix} x_1 + 2\pi j \\ x_2 \end{matrix} \right) = \int_{-1/2}^{1/2} w(\alpha, x) e^{2\pi i \alpha j} d\alpha, \quad x \in Q_H^{2\pi},$$

and that \mathcal{J} is unitary, i.e., its adjoint is its inverse. (The last integral in α abbreviates a dual evaluation.) Moreover, partial derivatives with respect to $x_{1,2}$ commute with \mathcal{J} , such that the Bloch transformed solution $w_B = \mathcal{J}u_T \in L^2((-1/2, 1/2); H_\alpha^1(Q_H^{2\pi}))$ satisfies the variational problem

$$\begin{aligned} & \int_{-1/2}^{1/2} \left[\int_{Q_H^{2\pi}} \nabla_x w_B(\alpha, \cdot) \cdot \nabla_x \overline{v_B} - k^2 w_B \overline{v_B} dx - \int_{\Gamma_H^{2\pi}} \overline{v_B} T_\alpha^+ w_B ds \right] d\alpha \\ & + \int_{Q_H^{2\pi}} [A_p - I_2] \nabla \mathcal{J}^{-1} w_B \cdot \nabla \overline{\mathcal{J}^{-1} v_B} - k^2 [1 - c_p] \mathcal{J}^{-1} w_B \overline{\mathcal{J}^{-1} v_B} dx \\ & = \int_{-1/2}^{1/2} \int_{\Gamma_H^{2\pi}} \mathcal{J}f(\alpha, \cdot) \overline{v_B}(\alpha, \cdot) ds d\alpha \end{aligned}$$

for all test functions $v_B \in L^2((-1/2, 1/2); H_\alpha^1(Q_H^{2\pi}))$ and a suitable right-hand side f defined via the incident field u^i ; T_α^+ are quasiperiodic Dirichlet-to-Neumann operators and $\Gamma_H^{2\pi} = (-\pi, \pi) \times \{H\}$, see [8]. Existence and regularity theory for this problem in, e.g., $L^2((-1/2, 1/2); H_\alpha^1(Q_H^{2\pi}))$ or in $H_{\text{per}}^r((-1/2, 1/2]; H_\alpha^1(Q_H^{2\pi}))$ can be deduced from the original surface scattering problem by equivalence. Moreover, the Galerkin discretization of this problem turns out to be attractive if one uses piecewise exponential ansatz functions in α as all integrals in α can be explicitly

computed. For details (e.g., for convergence results, details on the numerical implementation of the method and computational examples) we refer to [8], too.

REFERENCES

- [1] Simon Chandler-Wilde and Peter Monk, *Existence, uniqueness, and variational methods for scattering by unbounded rough surfaces*, SIAM Journal on Mathematical Analysis (2005) 37:598–618.
- [2] Julien Coatléven, *Helmholtz equation in periodic media with a line defect*, Journal of Computational Physics (2012) 231:1675–1704.
- [3] Housseem Haddar and Thi-Phong Nguyen, *A volume integral method for solving scattering problems from locally perturbed infinite periodic layers*, accepted for Applicable Analysis (2016).
- [4] Sonia Fliss and Patrick Joly, *Solutions of the Time-Harmonic Wave Equation in Periodic Waveguides: Asymptotic Behaviour and Radiation Condition*, Archive for Rational Mechanics and Analysis (2016) 219:349–386.
- [5] Armin Lechleiter, *The Floquet-Bloch transform and scattering from locally perturbed periodic surfaces*, Journal of Mathematical Analysis and Applications (2016), accepted.
- [6] Armin Lechleiter and Dinh-Liem Nguyen, *Scattering of Herglotz waves from periodic structures and mapping properties of the Bloch transform*, Proceedings of the Royal Society of Edinburgh Section A (2015), 231:1283–1311.
- [7] Armin Lechleiter and Ruming Zhang, *A convergent numerical scheme for scattering of aperiodic waves from periodic surfaces based on the Floquet-Bloch transform*, submitted (2016).
- [8] Armin Lechleiter and Ruming Zhang, *A Bloch transform based numerical method for scattering from locally perturbed periodic surfaces*, submitted (2016).

Participants

Dr. Tilo Arens

Fakultät für Mathematik
Karlsruher Institut für Technologie
(KIT)
76128 Karlsruhe
GERMANY

Prof. Dr. Liliana Borcea

Department of Mathematics
University of Michigan
530 Church Street
Ann Arbor, MI 48109-1043
UNITED STATES

Prof. Dr. Fioralba Cakoni

Department of Mathematics
Rutgers University
Busch Campus, Hill Center
Piscataway, NJ 08854-8019
UNITED STATES

Prof. Dr. David L. Colton

Department of Mathematical Sciences
University of Delaware
501 Ewing Hall
Newark, DE 19716-2553
UNITED STATES

Julian Eckhardt

Institut für Numerische
und Angewandte Mathematik
Universität Göttingen
Lotzestrasse 16-18
37083 Göttingen
GERMANY

Dr. Roland Griesmaier

Lehrstuhl für Mathematik IX
Mathematisches Institut
Universität Würzburg
Emil-Fischer-Strasse 40
97074 Würzburg
GERMANY

Dr. Housseem Haddar

Centre de Mathématiques Appliquées
École Polytechnique
91128 Palaiseau Cedex
FRANCE

Prof. Dr. Martin Hanke-Bourgeois

FB Mathematik/Physik/Informatik
Mathematisches Institut
Johannes-Gutenberg-Universität
55099 Mainz
GERMANY

Dr. Isaac Harris

Department of Mathematics
Texas A & M University
College Station, TX 77843-3368
UNITED STATES

Prof. Dr. Thorsten Hohage

Institut für Numerische
und Angewandte Mathematik
Universität Göttingen
Lotzestrasse 16-18
37083 Göttingen
GERMANY

Dr. Guanghui Hu

Weierstraß-Institut für
Angewandte Analysis und Stochastik
Mohrenstrasse 39
10117 Berlin
GERMANY

Dr. Nuutti Hyvoenen

Department of Mathematics
and Systems Analysis
Aalto University
P.O. Box 11100
00076 Aalto
FINLAND

Prof. Dr. Andreas Kirsch
Fakultät für Mathematik
Karlsruher Institut für Technologie
(KIT)
76128 Karlsruhe
GERMANY

Prof. Dr. Rainer Kress
Institut für Numerische
und Angewandte Mathematik
Universität Göttingen
Lotzestr. 16-18
37083 Göttingen
GERMANY

Prof. Dr. Armin Lechleiter
Zentrum für Technomathematik
FB 3, Universität Bremen
Postfach 330 440
28334 Bremen
GERMANY

Prof. Dr. Xiaodong Liu
Institute of Applied Mathematics
Chinese Academy of Sciences
No. 55 East Road, Zhongguancun
Beijing 100 190
CHINA

Prof. Dr. Peter Monk
Department of Mathematical Sciences
University of Delaware
Newark, DE 19716-2553
UNITED STATES

Prof. Dr. Shari Moskow
Department of Mathematics
Drexel University
Korman Center 269
3141 Chestnut Street
Philadelphia, PA 19104
UNITED STATES

Julian Ott
Fakultät für Mathematik
Karlsruher Institut für Technologie
(KIT)
76128 Karlsruhe
GERMANY

Prof. Dr. William Rundell
Department of Mathematics
Texas A & M University
College Station, TX 77843-3368
UNITED STATES

Prof. Dr. Otmar Scherzer
Computational Science Center
Universität Wien
Oskar-Morgenstern-Platz 1
1090 Wien
AUSTRIA

Prof. Dr. Virginia Selgas
Departamento de Matemáticas
Universidad de Oviedo, EPIG
C/Luis Ortiz Berrocal s/n
33203 Gijón
SPAIN

Prof. Dr. Samuli Siltanen
Department of Mathematics and
Statistics
University of Helsinki
P.O. Box 68
00014 University of Helsinki
FINLAND

Prof. Dr. John Sylvester
Department of Mathematics
University of Washington
Padelford Hall
Box 354350
Seattle, WA 98195-4350
UNITED STATES

Prof. Dr. Bastian von Harrach

Institut für Mathematik
Goethe-Universität Frankfurt
Postfach 111932
60054 Frankfurt am Main
GERMANY

Prof. Dr. Jun Zou

Department of Mathematics
The Chinese University of Hong Kong
Shatin
Hong Kong
CHINA